Striatopallidal cannabinoid type-1 (CB_1) receptors mediate amphetamine-induced sensitization

Yamuna Mariani[1,*], Ana Covelo[1,*], Rui S Rodrigues[1,*], Francisca Julio-Kalajzić[1], Antonio C Pagano Zottola[1,2], Gianluca Lavanco[1,3], Michela Fabrizio[1,4], Doriane Gisquet[1], Filippo Drago[5], Astrid Cannich[1], Jerome Baufreton[6], Giovanni Marsicano[1,7,#], Luigi Bellocchio[1,7,8,#]

[1] Univ. Bordeaux, INSERM, Neurocentre Magendie, U1215, F-33000 Bordeaux, France

[2] Institut de Biochimie et Génétique Cellulaires, UMR 5095, 33077 Bordeaux, France.

[3] University of Palermo, Department of Health Promotion, Mother and Child Care, Internal Medicine and Medical Specialties of Excellence “G. D’Alessandro”, 90127 Palermo, Italy

[4] Center for Interdisciplinary Research in Biology (CIRB), College de France, CNRS, INSERM, 5 Université PSL, 75231 Paris, France.

[5] Department of Biomedical and Biotechnological Sciences, Section of Pharmacology, University of Catania, Catania 95124, Italy

[6] Univ. Bordeaux, CNRS, IMN, UMR 5293, F-33000 Bordeaux, France.

[7] Corresponding authors, Giovanni Marsicano (giovanni.marsicano@inserm.fr), Luigi Bellocchio (luigi.bellocchio@inserm.fr)

[8] Lead contact

* these authors equally contributed to this work

[#] these authors share senior authorship

Twitter: @MarsicanoLab

SUMMARY

The repeated exposure to psychostimulants, such as amphetamine, causes a long-lasting enhancement in the behavioral responses to the drug, called behavioral sensitization[1]. This phenomenon involves several neuronal systems and brain areas, among which the dorsal striatum plays a key role[2]. The endocannabinoid system (ECS) has been proposed to participate in this effect, but the neuronal basis of this interaction have not been investigated[3]. In the CNS, the ECS exerts its functions mainly acting through the cannabinoid type-1 (CB_1) receptor, which is highly expressed at terminals of striatal medium spiny neurons (MSNs) belonging to both the direct and indirect pathways[4]. In this study, we show that, while striatal CB_1 receptors are not involved in the acute response to amphetamine, the behavioral sensitization and related synaptic changes requires the activation of CB_1 receptors specifically located at striatopallidal MSNs (indirect pathway). These results highlight a new mechanism of psychostimulant sensitization, a phenomenon that plays a key role in the health-threatening effects of these drugs.

RESULTS

Psychostimulants drugs like amphetamine directly enhance dopaminergic transmission. As a consequence, they temporarily increase movement, mental alertness, and attention inducing a sense of euphoria in humans, and trigger hyperlocomotion and stereotypies in rodents[5–7]. Interestingly, repeated administration of amphetamine is well known to induce a long-lasting enhancement of behavioral responses to the same dose of the drug, which is called sensitization[1]. This effect of amphetamine has been reliably

demonstrated for decades in several animal species[8]. Even though studies in humans are limited, it has been shown that repeated psychostimulant administration induces enhanced behavioral response, in a similar manner as in animal models[9]. In rodents, sensitization to amphetamine is generally assessed by measuring the intensity of the hyperlocomotor effect over the course of repeated administration of the drug, allowing the study of the complex underlying mechanisms[10–12]. Importantly, the neuronal changes accompanying sensitization have been hypothesized to, at least partially, underlie abuse and addiction to psychostimulants[6,13,14]. However, the mechanisms regulating the initiation and expression of behavioral sensitization are still under investigation.

The dorsal striatum has been identified as a key region for the motor-related effects of psychostimulants[2]. In particular, amphetamine injections have been shown to induce an increase of the dopaminergic tone within the dorsal striatum, resulting in hyperlocomotion through the modulation of the activity of the main cell type of this region, the medium spiny neurons (MSNs)[15–17]. The majority of MSNs belong to two different subpopulations according to their projection targets and/or their molecular identities: striatonigral neurons, also known as direct pathway MSNs (dMSNs), mainly characterized by the expression of the D1 dopamine receptor, and striatopallidal neurons, also defined as indirect pathway MSNs (iMSNs), identified by the expression of the D2 dopamine receptor. In the classical view of the basal ganglia (BG) these two pathways are proposed to work in an opposite and exclusive manner to coordinate motor behavior[18,19]. However, this model has been recently challenged. Indeed, new findings suggest a concomitant activity of these two neuronal populations for the correct execution of motor actions, which could underlie a joint regulation of

downstream circuits and behaviors[20–23]. Consistently, both populations have been shown to participate in the behavioral sensitization induced by amphetamine, even though with opposite outcomes[24,25]. Indeed, the transient blockade of the dMSNs impairs the expression of behavioral sensitization, while the inhibition of iMSNs enhances this behavior[25].

The endocannabinoid system (ECS) is formed by cannabinoid receptors (in the brain, mainly type-1 cannabinoid receptors, CB_1), their endogenous lipid ligands (endocannabinoids) and the machinery for the synthesis and degradation of endocannabinoids. The ECS has been involved in the response to psychostimulants and, particularly, in the expression of behavioral sensitization[3,26,27]. To date, sensitization is accompanied by increased endocannabinoid tone[3], and genetic or pharmacological manipulations of ECS activity modulate the expression of psychostimulants-induced sensitization[27,28]. Interestingly, striatal MSNs belonging to both neuronal populations, express one of the highest pools of the cannabinoid type-1 receptor (CB_1) in the brain[4,29]. However, the distinct role of CB_1 receptors located in dMSNs or iMSNs in mediating the behavioral sensitization has not been investigated yet. Thus, this study aimed at identifying the involvement of striatal CB_1 receptors in different striatal subpopulations in the expression of behavioral sensitization to amphetamine, and in the modulation of synaptic transmission induced by this drug of abuse in mice.

Generation of conditional mutant mouse lines lacking CB_1 receptors in striatal projecting neurons

In order to study the distinct roles of CB_1 receptors located in the different striatal pathways, we generated two new conditional mutant mouse lines,

bearing the deletion of CB_1 in the two distinct MSN populations, respectively. To delete the receptor in striatal D1-expressing (dMSN) or D2-expressing (iMSN) neurons, we crossed mice presenting the *CB_1* gene flanked by two loxP sites (*CB_1*-flox mice[30],) respectively with the Tg(Drd1a*cre)EY217Gsat mouse line or with the Tg(Adora2a*cre)KG139Gsat mouse line[31–34] . We named those two mouse lines Drd1-*CB_1*-KO and Adora2a-*CB_1*-KO, respectively.

To validate our model, we first determined whether the deletion of CB_1 was specific for the targeted population of MSNs. Hence, we performed a double-fluorescence *in situ* hybridization (FISH) staining, which allows the simultaneous labeling of mRNAs coding for CB_1 and D1, or of CB_1 and D2, and we measured the levels of colocalization in the dorsal striatum (**Figure 1A-C**). As expected, the colocalization between D1 and CB_1 was significantly reduced in Drd1-*CB_1*-KO mice, but not in Adora2a-*CB_1*-KO mice (**Figure 1A, B**). On the other hand, the number of D2(+) cells also expressing CB_1 was strongly reduced only in Adora2a-*CB_1*-KO mice (**Figure 1A, C**), indicating the specificity of our approach.

To further characterize these models, considering the developmental consequences of CB_1 deletion on striosomal/matrix organization[4,35], we performed an immunofluorescence quantification of μ-opioid receptors (MORs) and calbindin intensity (markers of striosome and matrix compartments, respectively) to check patch/matrix striatal organization[4,36] (**Figure 1D**). We observed no significant differences in the relative intensity of MOR and calbindin in Drd1-*CB_1*-KO and Adora2a-*CB_1*-KO mice (**Figure 1E, F**), suggesting that the structural organization of striatal compartments remains unaltered in these mutant mouse lines.

In neurons, the CB_1 protein is mainly presynaptic[37–40], and it is therefore found far from the cell body, where mRNA is enriched. Indeed, the highest levels of CB_1 immunoreactivity in the BG (and the whole brain) are found in the target regions of striatal neurons, such as the substantia nigra pars reticulata (SNr) and the external segment of the globus pallidus (GPe), which are the main post-synaptic targets of dMSNs and iMSNs, respectively[4,29]. To test whether the decreases in mRNA expression described above are reflected on changes in CB_1 protein levels, we first measured CB_1 protein levels by Western immunoblotting in the target regions. We found a specific reduction of CB_1 levels in the SN of Drd1-*CB1*-KO mice and in the GPe of Adora2A-*CB1*-KO mice, respectively (**Figure S1A**).

To easily detect the specificity of cre-dependent recombination, as well as the respective specific expression of CB_1 in the striatonigral and striatopallidal pathways, we then generated two new additional mouse lines in which CB_1 receptor is selectively re-expressed in D1(+) or Adora2a(+) cells over a knockout background. To this aim, we used the STOP-*CB1* mouse line, in which the expression of the CB_1 protein is prevented by the insertion of a STOP-cassette flanked by two loxP sites preceding the coding region of its gene, *Cnr1*[41,42]. Upon cre-mediated excision of the “STOP” cassette, the CB_1 receptor is re-expressed only in given cells, obtaining a conditional rescue (RS) mouse model[41,42]. We crossed the mouse lines used for the deletion of CB_1 (Drd1a*cre or Adora2a*cre) with the STOP-CB_1 mice, thereby generating Drd1-*CB1*-RS and Adora2a-*CB1*-RS mice (**Figure 1G**). This approach allows a direct identification of the recombination induced by the cre-lines on CB_1 expression. Fluorescent CB_1 immuno-labeling showed that both lines express CB_1

receptors in the dorsolateral striatum, with a stronger staining in Adora2a-*CB$_1$*-RS mice (**Figure 1H**). However, Drd1-*CB$_1$*-RS mice selectively express CB_1 in the SNr and partially in the GPe (**Figure 1H**), whereas Adora2a-*CB$_1$*-RS mice contain CB_1 in the GPe but not in the SNr (**Figure 1H**).

We previously showed that striatonigral CB_1 receptors (but not striatopallidal ones) mediate the cataleptic and antinociceptive effects of THC[43]. To test whether the genetic deletion of CB_1 bears a functional effect, we tested Drd1-*CB$_1$*-KO and Adora2a-*CB$_1$*-KO in the THC-induced tetrad assay, which consists in the analysis of four typical behavioral and somatic effects, namely catalepsy (assessed in the bar test), antinociception (hot-plate test), hypolocomotion (actimetry cages) and hypothermia[44]. Drd1-*CB$_1$*-KO mice were impaired in the cataleptic and antinociceptive effects of THC, while Adora2a-*CB$_1$*-KO mice were not different from controls (**Figure S1B**). The hypolocomotion and the hypothermia induced by the treatment were maintained in both genotypes (**Figure S1B**). These results confirm the functionality and selectivity of CB_1 deletion in striatal projection neurons in Drd1-*CB$_1$*-KO mice. Furthermore, our data indicate that the CB_1 deletion in Adora2a-*CB$_1$*-KO mice is specific for the indirect pathway, and confirm that this pool of receptors is not involved in the THC-induced tetrad assay (**Figure S1B**). Additional behavioral analyses showed that Drd1-*CB$_1$*-KO and Adora2a-*CB$_1$*-KO mice have normal motor coordination, sucrose preference, and object recognition memory despite a slight decrease of total exploration in Adora2A-*CB$_1$*-KO mice (**Figure S1C-E**). Overall, these results confirm that CB_1 receptors of the striatonigral pathway are sensitive to the cataleptic and antinociceptive effects of exogenous application of cannabinoid drugs, but striatopallidal CB_1

receptors are not involved in these typical short-term behavioral and somatic effects.

Taken together, these results indicate that the newly generated lines represent a suitable and functional tool to study the distinct role of CB_1 receptors located in striatal MSNs. Moreover, they confirm that CB_1 receptors of the striatonigral pathway are sensitive to the exogenous application of cannabinoid drugs, but striatopallidal CB_1 receptors are not involved in the typical short-term behavioral and somatic effects of these drugs.

CB_1 receptors in Adora2a-positive cells mediate amphetamine-induced behavioral sensitization

Psychostimulants, such as amphetamine, induce sensitization to their hyperlocomotor effect mainly by modulating dopaminergic signaling in the striatum[15,45] and CB_1 receptors have been proposed to be involved in these mechanisms[3,27]. To test whether amphetamine effects involve distinct striatal CB_1 receptor pools, we employed a behavioral protocol for evaluating the expression of the sensitization in Drd1-*CB_1*-KO and Adora2a-*CB_1*-KO mice undergoing repeated administration of amphetamine. Dose-response experiments in WT mice showed that, in our experimental conditions, only the dose of 5 mg/kg of amphetamine acutely induced a reliable hyperlocomotion in WT mice (**Figure S2A**), and was therefore chosen as dose for the repeated treatment.

Adora2a-*CB_1*-KO mice displayed a normal acute response to the drug at day 1 (**Figure 2A**), but they had impaired expression of the behavioral sensitization. Specifically, the repeated treatment induced a higher response to the drug in WT mice starting from the second injection, whereas we did not

observe a significantly increased response to amphetamine in Adora2a-*CB$_1$*-KO littermates (**Figure 2A**). Moreover, the locomotion of mutant mice at the 4th day of amphetamine and during the sensitization probe was lower than WT littermates, resulting in significantly reduced sensitization indexes (**Figure 2B, C**). Interestingly, Adora2a-*CB$_1$*-KO mice displayed no phenotype in basal locomotion, and they showed a normal habituation to the testing environment (**Figure S2B**). Furthermore, when mice were treated with saline during 4 days and with amphetamine as acute exposure at day 14, there were no differences between genotypes (**Figure S2C**), confirming that the phenotype of the mutants was specific for the sensitization process. Similarly, although low stereotypy rating was generally induced by amphetamine administration, no significant differences were observed between genotypes in the exhibition of stereotyped behaviors at day 1 (**Figure S3A-C**), day 4 (**Figure S3D-F**) and day 14 (**Figure S3G-I**), suggesting that the locomotor phenotype of the mutant lines is not indirectly caused by altered stereotypic responses. However, since the locomotor effects of psychostimulants depend on the behavioral state before the consumption of the drug[16], it is still possible that the phenotype was due to some basal difference between the genotypes. Thus, to better isolate the hyperlocomotion specifically induced by amphetamine, we calculated the difference in activity/min between the last period of habituation and the time after the injection (Δ activity, *see methods*). Also, this additional analysis confirmed that, although they responded like WT littermates to the first injection of amphetamine, Adora2a-*CB$_1$*-KO mice displayed a reduced response to amphetamine during the sensitization probe (**Figure 2D**). Taken together, these results indicate that CB_1 receptors in striatal Adora2a-expressing cells are not

involved in the effect of a single administration of amphetamine. Rather, they mediate the expression of behavioral sensitization and related molecular changes resulting from repeated administration of the psychostimulant.

CB_1 receptors in D1-positive cells are not involved in the behavioral sensitization induced by amphetamine

The direct or indirect pathways are largely interconnected, and their activation leads to an opposite regulation of output nuclei of the BG. However, they act in parallel for the correct execution of BG functions[22,46]. To investigate the impact of CB_1 receptors belonging to the direct pathway in the amphetamine-induced locomotor effect and sensitization, we tested the Drd1-*CB_1*-KO mice in our protocol. Drd1-*CB_1*-KO mice responded to amphetamine like their WT littermates, both regarding the acute effect and the sensitization (**Figure 2E-G**), as well as the induction of stereotyped behaviors (**Figure S3A-I**). Moreover, Drd1-*CB_1*-KO mice displayed normal basal locomotion and normal habituation to the testing chamber (**Figure S2D**), and they did not differ from WT littermates when they were treated with saline during 4 days, and with amphetamine at day 14 (**Figure S2E**). Δ activity analysis showed that Drd1-*CB_1*-KO mice had similar responses to amphetamine as their WT littermates, both at day 1 and day 14 (**Figure 2H**).

Several reports indicate that amphetamine sensitization is accompanied by specific changes in neuronal activity (measured by c-fos expression) according to the striatal sub-compartment involved (e.g., striosomes *vs* matrix)[47,48]. Thus, we wondered whether altered behavioral sensitization to amphetamine observed in Adora2A-*CB_1*-KO mice, was accompanied by differential changes in neuronal activity in the striatal compartments. We found that repeated

amphetamine was able to selectively increase the number of c-fos positive cells in the striosomes but not in the matrix, when compared to a single injection of the drug as previously reported[47,48]. Interestingly this effect only occurred in WT and Drd1-*CB1*-KO mice but not in Adora2A-*CB1*-KO mice (**Figure 2I and 2J**).

These data indicate that the amphetamine-induced behavioral sensitization and related changes in neuronal activity, specifically requires CB_1 receptors expressed by Adora2a-positive cells, whereas CB_1 receptors located in striatal D1-expressing cells are not involved in any analyzed effect of the drug.

Pathway-specific roles of CB_1 receptors

Even though the expression of the behavioral sensitization induced by amphetamine requires a normal activity of both direct and indirect striatal pathways[25], the data collected so far show that only CB_1 receptors located in Adora2a(+) cells are required for the effects of the repeated exposures to the drug, suggesting that only the indirect pathway is involved in this function of the endocannabinoid system. However, although striatopallidal MSNs are the major cell population expressing adenosine Adora2a receptors, they are widely distributed in the brain and in peripheral organs[49,50]. Therefore, the phenotype of Adora2a-*CB1*-KO mice does not allow to conclude that the cannabinoid control of the indirect pathway is the specific mechanism underlying the role of the endocannabinoid signaling in amphetamine sensitization. To address this issue, we used an intersectional recombinase approach[51] to specifically delete the CB_1 receptor in striatopallidal neurons[43]. Thus, we injected an adeno-associated virus (AAV) expressing the cre-recombinase in a flippase (FLP)-dependent manner (AAV-FRT-iCre-EGFP) into the striatum of CB_1-floxed mice. Simultaneously, we injected a retrograde AAV expressing the FLP (AAV-retro-

FLP-EBFP2) or a fluorescent marker as control (CTR, AAV-retro-EBFP2) into the GPe (**Figure 3A**). The injections were validated by histological expression analysis of the reporter proteins (**Figure 3B**), indicating that the approach is functional and, as previously shown[43], it allows the specific deletion of CB_1 from striatopallidal projecting neurons (ST-GPe-*CB_1*-KO). We have previously shown that in this approach the majority of EGFP labeled cells are also positive for D2R mRNA, resulting in a selective loss of CB_1/D2R co-expressing cells and a specific reduction of CB_1 immunoreactivity in the GPe when compared to the SNr[43]. ST-GPe-*CB_1*-KO mice displayed a very similar phenotype as Adora2a-*CB_1*-KO mice in amphetamine-induced sensitization. Indeed, they responded normally to the first injection of amphetamine, but they differed from control mice overall the repeated treatment (AAV effect; 2-way ANOVA) (**Figure 3C**). Consistently, we observed a significantly increased response to amphetamine only at day 14 in ST-GPe-*CB_1*-KO mice, while in CTR mice we observed a normal expression of the behavioral sensitization (**Figure 3C**). However, the sensitization index was reduced in ST-GPe-CB_1-KO mice only at day 4, with a trend for the sensitization probe at day 14 (p=0,063) when compared to control mice (**Figure 3D, E**). We did not observe differences in the basal locomotion and in the habituation to the testing chamber (**Figure S2F**). The analysis of the Δ activity indicated that there were no differences between the groups at day 1, but the sensitization probe was reduced in ST-GPe-*CB_1*-KO mice (**Figure 3F**).

Thus, the specific deletion of CB_1 in striatopallidal neurons impairs the expression of the behavioral sensitization induced by amphetamine. This evidence, complementary to the genetic manipulation of CB_1 receptors in Adora2a+ cells, strongly indicate that CB_1 receptors located in the indirect

striatal pathway are necessary for the complete expression of the behavioral sensitization induced by amphetamine.

Repeated amphetamine exposure increases amphetamine-sensitivity of striatopallidal neurons in a CB_1-dependent manner

Repeated treatments with amphetamine and the consecutive expression of behavioral sensitization are associated with transcriptional changes and hypersensitivity to dopamine[17]. However, the impact of the crosstalk between psychostimulants and the endocannabinoid system on synaptic properties of MSNs is still poorly investigated. To test whether amphetamine modulates synaptic transmission at striatopallidal synapses in a CB_1-dependent manner, we performed *ex vivo* patch-clamp recording experiments in Adora2a-*CB_1*-KO mice. For these experiments, we adapted the behavioral protocol to keep similar conditions (see methods for details). Mice received one injection of saline or amphetamine (5 mg/kg i.p.) during 4 consecutive days. At Day 14, animals were sacrificed and acute sagittal slices were collected (**Figure 4A**). Whole-cell recordings were made from prototypic GPe neurons, identified by immunostaining as FoxP2-negative[52] (**Figure S4A**), and the striatopallidal pathway was stimulated by placing a bipolar stimulating electrode in the striatum to evoke inhibitory postsynaptic currents (eIPSCs; **Figure 4B**). We measured the eIPSCs in basal conditions and after bath application of 1 µM amphetamine solution. In saline-treated mice, amphetamine induced a decrease in eIPSCs amplitude, and this effect seemed independent from CB_1 receptors, as it was present in both WT and Adora2a-*CB_1*-KO littermates (**Figure 4C, D**). Interestingly, we observed that amphetamine-mediated decrease in eIPSCs was blocked in the presence of sulpiride, a D2 receptor

antagonist (**Figure S4B, C**). Moreover, amphetamine application in slices of naïve mice reduced PPR, an effect blocked by the D2 antagonist (**Figure S4D, E**), indicating a presynaptic mechanism which given the low dopaminergic innervation of the GPe[53], suggests that amphetamine acts on the dopaminergic terminals onto iMSNs in the dorsal striatum. Application of amphetamine onto slices collected from amphetamine-treated mice caused a more pronounced decrease in eIPSCs amplitude in WT animals as compared to saline-treated WT mice (**Figure 4E, F**). Strikingly, this effect was completely abolished in Adora2a-*CB$_1$*-KO mice, where amphetamine was unable to induce any reduction of eIPSCs (**Figure 4E, F**). Interestingly, the analysis of the data in all experimental conditions, shows that *in vivo* repeated treatment with amphetamine caused a stronger reduction of the IPSCs induced by the acute application of amphetamine in WT mice, while there were no treatment-induced differences in Adora2a-*CB$_1$*-KO animals (saline vs amphetamine, **Figure 4G**). Moreover, there were no differences between genotypes when mice were treated with saline, but the reduction of IPSCs amplitude induced by the repeated treatment was impaired in Adora2a-*CB$_1$*-KO mice (WT vs KO, **Figure 4G**). These results suggest that the repeated treatment with amphetamine induces hypersensitivity to the drug reducing striatopallidal transmission, and this effect is mediated by CB_1 in this neuronal population.

Altogether, these data suggest that a CB_1-dependent synaptic "sensitization" of the indirect striatal pathway to amphetamine might at least partly explain the expression of the behavioral sensitization induced by amphetamine.

DISCUSSION

Using genetic manipulations in specific cell types combined with histological, behavioral, and electrophysiological approaches, this study shows in mice that CB_1 receptors located at striatopallidal and striatonigral neurons are dispensable for single exposure effects of amphetamine, but the former ones are necessary for behavioral and synaptic sensitization to the drug. Mice lacking CB_1 receptors in Adora2a(+) cells (marker of striatopallidal neurons, iMSNs) displayed a normal response to a single exposure to amphetamine, both behaviorally *in vivo* and electrophysiologically in striatopallidal *ex vivo* brain slices. In contrast, mutant mice displayed an impaired behavioral sensitization to amphetamine, while the deletion of CB_1 in Drd1(+) cells (marker for striatonigral neurons, dMSNs) did not affect this behavior. However, the role of CB_1 receptor in dMSNs in amphetamine sensitization, cannot be fully excluded, given the incomplete, although functional, deletion achieved in our Drd1-CB_1-KO mouse model.

Complementary to the general genetic manipulation in Adora2a(+) cells, the present data show that the viral deletion of CB_1 specifically in striatopallidal neurons leads to a similar phenotype, confirming that this pool of receptors is the one mediating the behavioral sensitization. Moreover, the *in vivo* treatment with amphetamine caused a synaptic sensitization in WT mice, with enhanced reduction of D2R-mediated striatopallidal IPSCs amplitude after bath application of the drug. Importantly, this effect was abolished in Adora2a-CB_1-KO mice, indicating that the synaptic and behavioral sensitization are underlined by a similar mechanism and, therefore, they might be causally linked.

In the classic view of the BG, direct and indirect pathways mutually antagonize their activity, exerting opposite effects on motor behaviors, with dMSNs facilitating and iMSNs inhibiting motor actions[54,55]. Several studies challenged this strict dichotomy, showing that both striatal pathways are activated during motor performances, suggesting that coordinate activity of both pathways guarantees correct execution of motor actions, with dopamine (DA) representing a fine modulator of these processes in physiological conditions[21,22,56]. Indeed, DA differentially modulates the balance of striatal pathways activation, stimulating dMSNs, which express G_s-coupled D1 dopamine receptor, and inhibiting iMSNs where it activates G_i-coupled D2 dopamine receptor[18]. In this study, we have shown that different pools of CB_1 receptors in the same brain region mediate different behaviors and neuronal adaptations acting on specific circuits. Thus, our data are relevant for the differential modulation of direct and indirect striatal neurons in response to psychostimulants.

Behavioral sensitization induced by psychostimulants in general, and amphetamine in particular, is a phenomenon studied since several decades, representing an important link between drug of abuse and pathophysiological changes in the brain. The dorsal striatum is a possible «target» for the sensitization, since many of the behaviors induced by amphetamine are often associated to an enhanced striatal DA release and modulation of MSN activity[11,17,57,58]. Activation of the endocannabinoid system (especially trough CB_1 receptor) has been proposed as one of the neuromodulatory mechanisms involved in the behavioral effects of psychostimulants, including addiction and sensitization[59,60]. Indeed, blockade of CB_1 receptors impairs sensitization, while

the selective rescue of CB_1 in MSNs partially restores this behavior[26,27]. Furthermore, artificial increase of endocannabinoid levels has also been shown to modulate amphetamine responses[28]. Our results show that CB_1 receptors located on striatopallidal (but not striatonigral) neurons is necessary for the expression of the behavioral sensitization to amphetamine without changing the response to the first exposure. However, other systems and many other mechanisms are known to participate in the behavioral sensitization to psychostimulants. For instance, μ and K opioid receptor have been shown to modulate amphetamine-induced sensitization in the striatum, the nucleus accumbens, and the VTA in a region-specific manner[61]. Even though the endocannabinoid system is not the only player in the sensitization, in this study we identified a specific pool of CB_1 receptors involved in the effects of amphetamine, underlying a differential involvement of striatal CB_1 receptors which could represent a more specific target of drugs of abuse. Psychostimulants effects require a normal activity of both populations of MSNs, and the reversible blockade of striatopallidal or striatonigral neurotransmission impairs the acute response to amphetamine and cocaine[62]. Furthermore, amphetamine-induced behavioral sensitization can be bidirectionally altered by chemogenetic inhibition of MSNs, (e.g., it is enhanced when striatopallidal neurons are inhibited, and abolished when the manipulation targets striatonigral neurons)[25]. Thus, we hypothesize that during the repeated treatment with amphetamine (but not upon single exposure), an orchestrated inhibition of striatopallidal neurons leads to activity-dependent physiological changes in the circuit, switching to a CB_1 dependent mechanism. Given the inhibitory role of these neurons on locomotor activity, this can provide ground for the expression

of the behavioral sensitization. On the other hand, since CB_1 receptors activity in striatonigral neurons seems not to be required for the sensitization, the regulation of this circuit during the repeated treatment could involve other systems. Given the complexity of BG connectivity, our study presents some limitations. For instance, a portion of dMSNs is known to send collaterals to the GPe[63], which are targeted by our viral deletion of CB_1. Thus, we cannot presently exclude the involvement of these collaterals in the phenotype observed in ST-GPe-CB_1-KO mice. Furthermore, the principal target of iMSNs is the GPe, but these neurons also send local collaterals in the striatum to dMSNs[64], modulating their activity. Thus, CB_1 receptors in iMSNs could impact the activity of both GPe neurons and dMSNs, thereby possibly participating in the behavioral sensitization to amphetamine.

The crosstalk between dopamine/psychostimulants and the ECS has been described in different brain regions. These include hippocampal formation, nucleus accumbens, amygdala and dorsal striatum[3,65–67]. The interaction between the two systems is crucial for the modulation of synaptic transmission and synaptic plasticity on corticostriatal projections (reviewed in [65]). In the dorsal striatum, the repeated treatment with amphetamine causes an increase in the production of endocannabinoid in vivo[3] , and their release is enhanced by the local treatment with a D2 dopamine receptor agonist[68]. Interestingly, cocaine is reducing striatal GABAergic transmission *via* D2 dopamine receptor, and this effect is blocked by a CB_1 receptor antagonist[67]. Furthermore, the amphetamine induces LTD on cortical projection, which is blocked by the CB_1 receptor antagonist AM251, and potentiated by the cannabinoid agonist WIN55212-2[66]. Thus, a tight crosstalk seems to exist between the endocannabinoid system

and dopaminergic transmission in the modulation of synaptic transmission and plasticity following psychostimulants treatment. In this *scenario*, we showed that CB_1 receptors in striatopallidal projections is necessary for the long-lasting inhibitory modulation of synaptic transmission induced by amphetamine. However, modulation of synaptic plasticity by psychostimulants has been mostly described in corticostriatal afferents. Therefore, long-term amphetamine effects on striatopallidal transmission could be either consequence of previous neurobiological changes happening in this circuit, and/or an additional modulatory process of striatopallidal transmission mediated by DA and CB_1 receptors. Further studies are required to better investigate the interaction between corticostriatal and striatopallidal plasticity, with synaptic changes induced by psychostimulants.

In summary, CB_1 receptors located at striatopallidal neurons are involved in the expression of the behavioral sensitization and related synaptic changes induced by amphetamine, representing a new specific target for drugs of abuse which involve distinct regulation of striatal pathways.

ACKNOWLEDGMENTS

This study is dedicated to the memory of our friend and colleague, Federico Massa. We thank Delphine Gonzales, Nathalie Aubailly, Elisabeth Huc and all of the personnel of the Animal/Genotyping Facility of the NeuroCentre Magendie for mouse breeding and care. We also thank all of the members of the Marsicano lab for useful discussions and Virginie Morales for invaluable help with administrative work. We thank Rosmara Infantino for help in mice sacrifices. We thank the Histology and Biochemistry platforms of the NeuroCentre Magendie, as well as the Bordeaux Imaging Center (BIC) for help in the experiments. We thank, Veronique Deroche, Jean-Francois Fiancette, Francis Chaouloff and Daniela Cota for help in providing reagents as well as for their useful and critical reading of the manuscript. We thank Anna Beyeler for the help in artworks and the useful and critical reading of the manuscript. We thank Stéphanie Caillé-Garnier for the help in assessing behavioral stereotypies. This work was supported by Inserm (to G.M. and L.B.); EU–FP7 (PAINCAGE, HEALTH-603191, to G.M.); the European Research Council (Endofood, ERC–2010–StG–260515; CannaPreg, ERC-2014-PoC-640923; Micabra, ERC-2017-AdG-786467, to G.M.); Fondation pour la Recherche Medicale (DRM20101220445, to G.M., and ARF20140129235, to L.B.); the Human Frontiers Science Program (to G.M.); Region Aquitaine (to G.M.); French State/Agence Nationale de la Recherche (LABEX BRAIN ANR-10-LABX-43, to G.M. and JCJC MitoCB1-fat, to L.B.) and the French government in the framework of the University of Bordeaux's IdEx "Investments for the Future - France 2030" program / GPR BRAIN_2030 (to J.B., G.M. and L.B.).

AUTHOR CONTRIBUTION

Y.M., R.S.R., M.F., F.D. and G.L. performed and analyzed the behavioral experiments. A.C. and J.B. performed and analyzed the electrophysiological experiments. Y.M., R.S.R., F.J.-K., D.G., A.Cannich, and A.C.P.Z. performed and analyzed the anatomical and histological experiments. Y.M., G.M., and L.B. conceived and supervised the whole project and wrote the manuscript. All of the authors edited and approved the manuscript.

DECLARATION OF INTERESTS

The authors declare no competing interests.

FIGURE LEGENDS

Figure 1. Conditional mutant mouse lines for studying striatal CB_1 receptors.

A) Representative micrographs of double-fluorescent in situ hybridization experiment. D1 or D2 receptors (green), and CB_1 receptors (red), coding genes expression in the dorsal striatum of Drd1-*CB_1*-KO and Adora2a-*CB_1*-KO mice, compared to their WT littermates. Left: lower magnification of the entire striatum. Scale bar = 300 µm. Right: high magnification of dorsolateral portion where the co-expression was analyzed. Scale bar = 50 µm.

B) Relative quantification of D1/CB_1 co-expression in all genotypes (% of WT).

C) Relative quantification of D2/CB_1 co-expression in all genotypes (% of WT).

D) Immunofluorescence against MOR (red) and Calbindin (green) in the dorsal striatum of WT, Drd1-*CB_1*-KO, and Adora2a-*CB_1*-KO mice. Scale bar = 50 µm.

E - F) Relative quantification of MOR and calbindin intensity, respectively (% of WT).

G) Schematic for the selective rescue of CB_1 receptors.

H) Immunofluorescence against CB_1 receptors in STR, GPe, and SNr of Drd1-*CB_1*-RS and Adora2a-*CB_1*-RS mice.

For details of statistical analysis, see **Table S1**. See also **Figure S1**.

Figure 2. CB_1 receptors in striatopallidal neurons mediate amphetamine-induced sensitization.

A) Effects of the repeated treatment with amphetamine (5 mg/kg i.p.) on total activity (events/h) in Adora2a-*CB_1*-KO mice.

B) Sensitization index, calculated as the relative change in the total activity at Day 4 respect to Day 1, in Adora2a-*CB$_1$*-KO mice.

C) Sensitization index, calculated as the relative change in the total activity at Day 14 respect to Day 1, in Adora2a-*CB$_1$*-KO mice.

D) Δ activity (events/min) calculated for the first exposure to amphetamine (Day 1) and the sensitization probe (Day 14). Differences between Adora2a-*CB$_1$*-KO and their WT littermates (i.e., CB1-flox littermates without Cre expression) are observed at Day 14.

E) Effects of the repeated treatment with amphetamine (5 mg/kg i.p.) on total activity (events/h) in Drd1-*CB$_1$*-KO mice.

F) Sensitization index, calculated as the relative change in the total activity at Day 4 respect to Day 1, in Drd1-*CB$_1$*-KO mice.

G) Sensitization index, calculated as the relative change in the total activity at Day 14 respect to Day 1, in Drd1-*CB$_1$*-KO mice.

H) Δ activity (events/min) calculated at Day 1 and Day 14 show no differences between WT and Drd1-*CB$_1$*-KO mice.

I) Immonofluorescence against MOR (red) and c-Fos (green) in the dorsal striatum of WT, Drd1-*CB$_1$*-KO, and Adora2a-*CB$_1$*-KO mice under saline and amphetamine (5 mg/kg i.p.) treatments. Scale bar = 50 μm.

J) Relative quantification of c-Fos positive cells in striosomes (left) and matrix (right) compartments. Differences in c-Fos expression in striosomal compartments between saline- and amphetamine-treated WT and Drd1-*CB$_1$*-KO, but not Adora2a-*CB$_1$*-KO, mice.

For details of statistical analysis, see **Table S1**. See also **Figures S2-S3**.

Figure 3. Viral deletion of CB_1 in striatopallidal neurons (ST-GPe) reduced the sensitization induced by amphetamine.

A) Schematic representation of the double-viral strategy; STR: Striatum, GPe: external segment of Globus Pallidus.

B) Representative images of the injection sites; Top: Striatal expression of EGFP indicates recombination FLP-dependent, and expression of the Cre-recombinase; Bottom: GPe from mice injected with the retrograde flippase expression virus (FLP), or control virus. Scale bar = 200 μm.

C) Effects of the repeated treatment with amphetamine (5 mg/kg i.p.) on total activity (events/h) in ST-GP-*CB_1*-KO mice, compare to control mice.

D) Sensitization index, calculated at Day 4, in CTR and ST-GPe-*CB_1*-KO mice.

E) Sensitization index, calculated at Day 14, in CTR and ST-GPe-*CB_1*-KO mice.

F) Δ Activity/min from Day 1 and Day 14 showing differences between groups at Day 14.

For details of statistical analysis, see **Table S1**. See also **Figures S2-S3**.

Figure 4. Repeated amphetamine exposure increases amphetamine-sensitivity of the striatopallidal pathway in a CB1-dependent manner.

A) Experimental timeline: Mice were i.p. injected with either saline or amphetamine for 4 consecutive days. At Day 14 mice were sacrificed and patch-clamp recordings were performed.

B) Scheme (left) and DIC image (right) depicting the experimental approach. Striatum (Str), Globus Pallidus capsula externa (GPe), anterior comisure (a. c.). Scale bar = 250 μm.

C) Representative IPSC traces recorded in basal conditions and after bath application of 1µM amphetamine from WT and Adora2a-*CB$_1$*-KO mice treated with saline. Scale bars: 100 pA, 20 ms.

D) Time course of bath-applied amphetamine on IPSC amplitude in WT and Adora2a-*CB$_1$*-KO mice treated with saline.

E-F) Time course of bath-applied amphetamine on IPSC amplitude in WT and Adora2a-*CB$_1$*-KO mice treated with amphetamine.

G) Change in IPSC amplitude recorded 20min after bath application of amphetamine in all experimental conditions.

For details of statistical analysis, see **Table S1**. See also **Figure S4**

STAR METHODS

Resources availability

Lead contact

Further information and requests for resources and reagents should be directed to and will be fulfilled by the lead contact, Luigi Bellocchio (luigi.bellocchio@inserm.fr).

Materials availability

This study did not generate new unique reagents.

Data and code availability

- The datasets used to generate figures from the present study have not been deposited in a public repository but are available on request from the lead contact.
- This paper does not report original code.
- Any additional information required to reanalyze the data reported in this paper is available from the lead contact upon request.

Experimental models and study participant details

Experiments were approved by the Committee on Animal Health and Care of INSERM and the French Ministry of Agriculture and Forestry (authorization number 3306369) and the French Ministry of Higher Education, Research and Innovation (authorization APAFIS#23810). Mice were maintained under standard conditions (food and water *ad libitum*; 12h/12h light/dark cycle, light on 7 a.m.; experiments were performed between 9 a.m. and 5 p.m.). Grouped-

housed male mice, between 8 to 12 weeks old, were used for this study. *CB_1*-flox mice, generated and maintained as describe before [30,69,70], were used for the generation of conditional mouse lines and for the viral deletion experiment. Conditional CB_1 mutant mice and their WT littermates were generated by a 3-step breeding scheme using the Cre-loxP system and maintained in our animal facility.

Adora2a-CB_1*-KO:* to generate the Adora2a-*CB_1*-KO line, *CB_1*-flox mice were crossed to Adora2a-cre mice (Tg(Adora2a-cre)KG126[32]); in Adora2a-cre mice, provided by MGI (Jackson Laboratory, USA), the cre recombinase was placed under the control of adenosine A2A receptor gene (*Adora2A*) regulatory sequences using BAC transgenesis.

Drd1-CB_1*-KO:* similarly as describe above, *CB_1*-flox mice were crossed to Drd1-cre mice (Tg(Drd1-cre)EY217), in which the cre recombinase is inserted in the regulatory sequence of the dopamine receptor d1 gene (*Drd1a*[32]), provided by MGI (Jackson Laboratory, USA).

WT controls for each of these 2 lines were *CB_1*-flox littermates without cre expression.

Adora2a-CB_1*-RS and Drd1*-CB_1*-RS:* transgenic mice were generated with the same approach described before [41], by crossing Adora2a-Cre and Drd1-Cre with Stop-*CB_1* mice. Upon CRE deletion in Adora2A or Drd1 positive cells, stop-cassette was excised driving selective CB_1 re-expression.

Methods details

Drugs

THC was obtained from THC Pharm GmbH (Frankfurt, Germany). Used at 10mg/kg, it was dissolved in a mixture of saline (0.9% NaCl) with 5% ethanol and 4% cremophor. D-amphetamine sulfate (Tocris, UK, cat 2813) was kindly provided by Véronique Deroche, dissolved in saline (0,9% NaCl) and injected at 1, 2.5 and 5 mg/kg. Vehicles contained the same amounts of solvents respectively to the drug. All drugs were prepared fresh before the experiments.

Viral Vectors and surgery procedures

For the striatopallidal CB_1 deletion experiment we used the same procedures we described before[43]. Briefly, mice were anesthetized by inhalation of isofluorane 5% and placed into the stereotaxic apparatus with the anesthesia maintained at 2% during the entire surgery. AAV vectors were injected with the help of a microinjector (Nanoject III, Drummond Scientific, PA, USA). The deletion was performed injecting, in the dorsal striatum (STR), the viral vector AAV-hEF1a-dFRT-iCre-EGFP (titre $6.3*10^{12}$, 2 injections of 1µl per side) with the following coordinates: AP + 0,8 ML ± 2,0 DV -3,0 and -3,5. The retrograde vectors AAV-retro-hSyn1-EBFP2-FLPo ($6.4*10^{12}$) or AAV-retro-hSyn1-EBFP2 ($4.1*10^{12}$) were injected in the external Globus Pallidus, GPe (AP – 0,5 ML ± 1,8 DV – 4,25; volume 350 nl per side). The viral vectors were purchased from the Viral Vector Facility (VVF) of the Neuroscience Center Zurich (Zentrum für Neurowissenschaften Zürich, ZNZ). Animals were allowed to recover for at least four weeks before the beginning of behavioral experiments, and at the end of the protocol they were fixed by transcardial perfusion of 4% PFA. The brains were frozen in isopentane, 30µm slices were collected with the help of a

cryostat (Microm HM 500M Microm Microtech) and then processed for imaging to detect EBFP2 and EGFP. Mice that did not fulfill histological positive criteria were excluded from the study.

Immunofluorecence and Double fluorescent in-situ hybridization (FISH)

For the anatomical experiments, Adora2a-*CB_1*-KO/RS and Drd1-*CB_1*-KO/RS mice were sacrificed by transcardial perfusion with 20 mL PBS pH7.5 following by 30 mL 4% PFA. After overnight (ON) post fixation, in the same fixative, the brains were embedded in 30% sucrose for cryopreservation. Few days later, brains were frozen in cold isopentane (-60°C) and 30 µm thick cryosections were cut in a cryostat (Leica, CM1950S), they were collected and stored at -20°C, in antifreeze solution [in 0.2M phosphate buffer $H_2PO_4^-/HPO_4^{-2}$: 20% v/v glycerol; 30% v/v Ethylene glycol] until further use.

Immunofluorescence: *CB_1 receptor* – The immunodetection of CB_1 receptor was done by incubating slices ON at 4°C with the primary antibody directed against CB_1 receptor, rabbit anti CB_1 (1:500, CB_1-Rb-Af380; frontier institute, Japan), and revealed by incubating 2h at room temperature (RT) with the secondary antibody Goat anti Rabbit Alexa Fluor 488 (1:500, A110008, Invitrogen, United States). *Calbindin, c-fos and mu opioid receptor (MOR)* – The immunodetection of calbindin, c-Fos, and MOR was done by incubating ON at 4°C with the primary antibody directed against calbindin, mouse anti-Calbindin-D-28K (1:1000, C9848; Sigma Aldrich, United States) and MOR, rabbit Anti-Mu Opioid Receptor (1:4000, ab134054 Abcam, Cambridge, UK), or against c-Fos, guinea-pig anti-c-Fos (1:1000, 226 005, Synaptic Systems, Göttingen, Germany) and revealed by incubating 2h at RT with the secondary

antibodies Donkey anti Mouse Alexa Fluor 488 (1:500, A-21202, Invitrogen, United States), Goat anti Guinea pig Alexa Fluor 488 (1:500, A-11073, Invitrogen, United States) and Goat anti Rabbit Alexa Fluor 594 (1:500, A11012, Invitrogen, United States). *Forkhead-Box P2 (FoxP2) and biocytin* – After electrophysiological recordings in acute slices from Adora2a-CB_1-KO mice and their WT littermates, the slices were fixed overnight in a solution of 4% PFA and maintained in PBS at 4°C, until FoxP2/biocytin immunostaining. FoxP2 was immunodetected by the primary antibody Rabbit anti-FoxP2 (1:4000, ab16046 Abcam, Cambridge, UK) ON at 4°C and revealed by 2h of RT incubation with Donkey anti-Rabbit Alexa Fluor 488 (1:500, A21206, Invitrogen, United States). The recorded neurons were filled with biocytin and, in order to stain them, the slices were incubated 4h at RT with NeutrAvidin Protein, DyLight 633 (1:500, 22844, Invitrogen, United States). The recorded neurons positive for the staining against FoxP2 were excluded from the analysis. All immunostaining were imaged with a confocal Leica SP8 microscope 40x objective (Leica, Germany). Image analyses and counting was performed through ImageJ software bilaterally in two 40x images per striatum, restricted to the dorsolateral area; per mouse, at least 5 striatal slices were analyzed (total of 10 images per condition). For calbindin and MOR quantification, relative immunoreactivity was measure and expressed as percentage of WT slices. For c-Fos quantification, counts were normalized to the area occupied by striosome/matrix structures as previously described[48]. To calculate the density of c-Fos positive cells in striosomes and matrix, the number of cells in the “patch” regions were counted and subtracted from the total number of cells, and patch area was subtracted from the total area; the same procedure was done to the number of cells in

matrix regions. c-Fos counts were expressed as the number of Fos-positive cells per normalized area (mm^2).

In situ hybridization (FISH): double FISH experiments to measure the number of CB_1/D_1R vs CB_1/D_2R positive striatal neurons, were carried as previously described[43,71,72] with some modifications. Briefly, after inactivation of endogenous peroxidases, sections were hybridated with a combination of coupled Digoxigenin (FITC)-labeled riboprobe against mouse CB_1 receptor (1:1000, prepared as described in [73]) together with DIG riboprobe against D1R or D2R (1:1000,[74]). The probes were revealed one after the other by incubating 2h at RT with the antibody sheep anti FITC-POD (1:1500, Roche, 11426346910) following by a TSA reaction with cyanine 3 (Cy3)-labeled tyramide (1:100 for 10 minutes, Akoya biosciences NEL744001KT) in order to detect CB_1 receptor. Posterior to the inactivation of remaining active peroxidases coupled to sheep anti FITC-POD, the second probe was spotted by incubating ON at 4°C with the antibody sheep anti DIG-POD (1:1500, Roche, 11207733910) following by a TSA reaction using fluorescein (FITC)-labeled tyramide (1:100 for 10 minutes, Akoya biosciences NEL741001KT) for D_1R or D_2R receptor. Sense control probes were used to establish background signal. Finally, the sections were mounted, cover slipped and imaged with a confocal Leica SP8 microscope 40x objective (Leica, Germany). Counting of co-expressing cells was performed manually as previously described[43,71,72]. Image analyses and counting was performed bilaterally in two 40x images per striatum, restricted to the dorsolateral area; per mouse, at least 3 striatal slices were analyzed. This resulted in counting 400-600 neurons in average per each condition/analysis.

Western Blot for CB1R in GPe and SN tissue homogenates

For this experiment, naive, Adora2a-CB1-KO, Drd1-CB1-KO mice and their respective WT littermates were used. Immediately after cervical dislocation, the brain was extracted, the external globus pallidus (GPe) and the substancia nigra (SN) were rapidly dissected using the coronal brain matrix, and processed as described before[75,76]. Tissue samples were immediately frozen in dry ice and stored at -80°C. Samples were then homogenized using the Tissue Lyser (Quiagen, Hilden, Germany), in lysis buffer (0.05M Tris-HCl pH 7.4, 0.15M NaCl, 0.001M EDTA, 10% Glycerol, 1% Triton X-100) added with protease and phosphatase inhibitors purchased from Roche (Basel, Switzerland). After 10 min incubation at 4°C, samples were centrifuged at 17000 g for 20 min at 4°C. Bradford protein assay was performed on the solubilized fractions for measuring protein contents. Samples were then mixed with denaturing 4x Laemmli loading buffer (250 mM Tris-HCl, 40% Glycerol, 8% SDS, 5% β-Mercaptoethanol, 0.2% Bromophenol blue) and heated at 37°C for 30 minutes. Samples were analyzed on 4-20% precast polyacrylamide gels (Bio-Rad, Hercules, California) and transferred onto PVDF membranes 0.45µm (Merk Millipore, Burlington, MA). Membranes were blocked in a mixture of Tris-buffered saline and polysorbate 20 (20mM Tris-HCl pH 7.6, 150mM NaCl, 0.05% Tween 20) containing 5% of non-fat dry milk for 1 h at RT. For the immunoblotting the antibody against CB_1 (ab23703; 1:200, 1h RT, Abcam, Cambridge, UK) and tubulin (sc-69969; 1:5000, 1h at RT, Santa Cruz Biotechnology, Dallas, Texas) were used. The signal was detected with HRP-linked antibodies (1:2000, Cell Signaling Technology, Danvers, MA) and visualized by enhanced chemiluminescence detection (Clarity Western ECL

Substrate, Bio-Rad, Hercules, California). The images have been acquired on ChemiDoc Touch (Bio-Rad, Hercules, California) and analyzed using the Image Lab software (Bio-Rad, Hercules, California).

Behavioral tests

THC-induced tetrad assay: 30 min after the injection of THC (10 mg/kg, i.p.) mice were successively tested for hypothermia, antinociception, catalepsy and locomotion[44,74]. Hypothermia is expressed as the difference in the body temperature, measured before and after the injection by rectal probe thermometer. For measuring the locomotion, mice were placed in a single actimetry cage (Imetronic, France) equipped by infrared beams, for 5 min. For the catalepsy, mice were placed in a new cage without bedding with on a horizontal bar (0.7cm Diameter) placed at 4.5 cm high. Mice were positioned with the fore paws gripping the bar and the hind paws in the plastic box. The time of immobility spent in this position was scored for two minutes. Immediately after, mice were placed in a Hot Plate (BIOSEB) to measure antinociception. The plate was pre-heated at 52°. The escape latency, defined as the time until the mice showed signs of discomfort (paw licking, jumping), was recorded. All equipment was cleaned with ethanol 25% and dried with paper towels between all the trials.

Rotarod test: for testing the motor coordination and motor skills learning, mice were placed with all four pawns on a turning horizontal bar of 3 cm diameter, placed 30 cm above the bottom of the apparatus (RotaRod LE8200, Harvard Apparatus). The bar rotates around its longitudinal axis with constant acceleration, from 4 to 40 rpm/min over 600s. The latency to fall was scored and the procedure is repeated over 3 trials by day, during 3 consecutive days.

Sucrose preference test: the test took place in the home cage. For this test mice were habituated to drink from two 50ml-drinking tubes (Conical Centrifuge Tube, Thermo Fisher Scientific, Rochester, USA) filled with water. Consumption was measured by controlling for spillage. To avoid any neophobic behavior during the test phase, one drinking tube was replaced with another identical tube filled with water solution of 5% sucrose, for 1h by day. The procedure was repeated during 2 days, alternating the position of the sucrose. After the habituation, mice were water deprived and they were trained to drink only one hour per day, during three consecutive days. The day of the test, two drinking tubes were presented simultaneously, one filled with water and the second one with sucrose. Mice were allowed to drink during 1h and the preference was measured as the ratio between sucrose consumption over the total consumption.

Novel object recognition memory test: for testing whether our models are not impaired in hippocampal memory formations we performed the novel object recognition memory test (NOR), as describe before [77]. The task took place in L-shaped maze made of dark gray polyvinyl chloride shaped by two identical perpendicular arms (35 cm and 30 cm long respectively for external and internal L walls, 4.5 cm wide and 15 cm high walls) placed on a white background. The task consisted of 3 sequential daily session of 9 min each. During the habituation session (day 1), mice were allowed to freely explore the maze in the absence of any objects. For the acquisition session (day 2) two identical objects were positioned at the extremities of each arm. The memory test occurred 24 h later (day 3), in which one of the familiar objects was replaced by a novel object different in its shape, color, and texture. The position of the novel

object and the associations of novel and familiar were randomized. Apparatus and objects were cleaned with ethanol (70%) before experimental use and between each animal testing. Memory performance was assessed by the discrimination index (DI). The DI was calculated as the difference between the time spent exploring the novel (TN) and the familiar object (TF) divided by the total exploration time (TN+TF): DI = [TN-TF]/[TN+TF]. Object exploration was defined as the orientation of the nose to the object at a distance of less than 2 cm. Experienced investigators evaluating the exploration were blind to the genotype of the animals.

Amphetamine-induced behavioral sensitization: for the measure of locomotor effects induced by amphetamine, we used the Actimeter apparatus (Imetronic, Marcheprime, France). Apparatus: the Actimeter consists in an aluminium ventilated rack covered with PVC plates. The rack contains 8 single boxes (actimetry cages), 30x16x11cm. Each box is equipped with infrared sensors to detect locomotory activity, and infrared planes to detect rearings. The rack is connected with electronic interface, which provides the formatting of signals from infrared sensors and allows communication with the computer. The locomotory activity is recorded as beam-breaks. Protocol: every day of the test, mice are moved in the testing room and they are allowed to adapt to the room for at least 45 minutes. After this period mice are located in a single box and their basal locomotion is recorded for 1h period (Habituation). Once the habituation ends, mice receive amphetamine (5 mg/kg, i.p.), and their locomotion is recorder for another 1h period (Test). The same identical procedure is repeated over 4 consecutive days. Mice were rested for 10 days, and at day 14 (sensitization probe), the same procedure is repeated. Data: the

software Imetronic store the data as beam-breaks/5 min unit. The locomotory activity is then expressed as Activity/h, corresponding to the total activity during 1h recording, or as Δ activity/min. For this measure we calculate the activity/min during the last period of the habituation phase (range of time in which the locomotion induced by the novel environment exploration is lower) and we subtracted it to the activity/min recorded during the total post-injection period. Finally, for the individual analysis of the sensitization we calculate the «sensitization indexes», as the relative change in the activity/h between Day1 and Day4 {(D4-D1)/(D1)} and Day14 {(D14-D1)/(D1)}.

Stereotyped behaviors: for assessing the presence of stereotyped behaviors upon our protocol of amphetamine-induced behavioral sensitization, we kept conditions similar to those of the sensitization protocol. For this purpose, we used single Plexiglass boxes (30x16x11cm) and the behavior of the mouse was recorded by a horizontal camera. Every day of the experiment, mice were moved to the testing room and allowed to adapt for at least 45 minutes. After this period, mice were located in a single box for 30 mins on day 1 and 15 minutes the following days (habituation). Once the habituation ended, mice received a single injection of saline or amphetamine (5 mg/kg, i.p.), and were placed back in the single box for 1h period (test). The procedure was repeated over 4 consecutive days. Mice rested for 10 days and at day 14 the same procedure was repeated, with all groups receiving amphetamine (5 mg/kg i.p.). Mice stereotyped behaviors were rated offline by experimented investigators blind for genotype and treatment. Stereotypies from day 14 were scored every 10 mins of the test and averaged using a previously described scale[78]. Scores were defined as follows: 0=inactive, 1=intermittent activity, 2=continuous

activity, 3=intermittent stereotypy, 4=continuous stereotypy over a wide area including stereotyped locomotor activity, sniffing and rearing, 5=continuous stereotypy over a restricted area (mainly sniffing and rearing), 6=pronounced continuous stereotypy in a restricted area (mainly sniffing), 7=intermittent licking or biting, 8=continuous licking or biting.

Saline and amphetamine treated-mice were fixed by transcardial perfusion 90 minutes after the amphetamine injection at day 14 in order to see the effects of the drug on neuronal activity (by c-fos immunostaining) in the striosomes vs the matrix.

Electrophysiology

Adora2a-*CB$_1$*-KO mice and their WT littermates were placed in a dark arena (30x16x11cm), and let to habituate to the environment for 15 minutes. After this period, animals were i.p. injected with either saline or 5 mg/kg amphetamine and their locomotion was recorded for 45 minutes period. The same procedure was repeated for 4 consecutive days. At day 14 animals were decapitated and the brain was rapidly removed and placed in ice-cold cutting solution that contained (in mM): sucrose 180, KCl 2.5, NaH2PO4 1.25, NaHCO3 26, MgCl2 12, CaCl2 0.2, glucose 11, and was gassed with 95% O2/5% CO2 (pH = 7.3–7.4). 350 µm thick sagittal slices were made with a vibratome (VT1200S, Leica) and incubated in ACSF at 34ºC, after 30 min slices were kept at RT. ACSF contained (in mM): NaCl 123, KCl 2.5, NaH2PO4 1.25, NaHCO3 26, MgCl2 1.3, CaCl2 2.5, and glucose 11, and was gassed with 95% O2/5% CO2 (pH = 7.3–7.4). Slices containing the striato-pallidal pathway were transferred to an immersion recording chamber, superfused at 2 ml/min with gassed ACSF and visualized under an Olympus microscope (Olympus Optical).

Electrophysiological recordings of GPe neurons were made in whole-cell configuration of the patch-clamp technique. Patch electrodes had resistances of 4–6 MΩ when filled with the internal solution containing (in mM): KCl 130, HEPES 10, EGTA 1, MgCl2 2, CaCl2 0.3, Phosphocreatin 7, Mg-ATP 3, Na-GTP 0.3 and 1% biocytin (pH = 7.3, 290 mOsm). Recordings were obtained with a MultiClamp 700B amplifier (Molecular devices). Membrane potential was held at −70 mV and series and input resistances were monitored throughout the experiment using a −5 mV pulse. Cells were discarded when series and input resistances changed >20%. Signals were fed to a PC through a DigiData 1440A interface board. Signals were filtered at 1 KHz and acquired at 10 KHz sampling rate. The pCLAMP 10.7 (Axon instruments) software was used for stimulus generation, data display, acquisition and storage.

Platinum/iridium bipolar parallel stimulation electrodes (1 mm electrode spacing) were placed in the striatum for bipolar stimulation of the striato-pallidal pathway. Paired pulses (50 ms interval) were continuously delivered at 0.33 Hz using a Digitimer Ltd stimulator. Evoked inhibitory postsynaptic currents (IPSCs) were isolated in the presence of NBQX (10 µM) and AP-5 (50 µM) to block AMPA and NMDA receptors, respectively. Stable IPSCs were recorded for 5 min in basal conditions and amphetamine 1µM was added in the bath for additional 20 min. After the experiments were finished, the patch pipette was gently removed and slices were fixed in PFA 4% at 4ºC overnight, then, they were moved to PBS and stored at 4ºC for immunohistochemistry.

IPSC amplitude was normalized to the 5 min of basal recordings and time bins of 60 s were made to illustrate the time course of amphetamine effects. The effects of amphetamine on IPSC amplitude on the different experimental groups

were determined by comparing the last 5 min of recordings (averages of n = 100 IPSCs). GPe projecting neurons are divided into two types of neurons, called arkypallidal and prototypic, which differ for their connections[52,79]. Since we are interested in studying the synaptic transmission of the striatopallidal pathway, we limited the analysis at prototypic neurons, target of iMSNs[79]. To this aim, we filled the recorded neurons with biocytin and we performed immunostaining against the protein Forkhead-Box P2 (FoxP2; marker for arkypallidal neurons, *see before*), the recorded neurons positive for the staining were excluded from the analysis. In another set of experiments, electrophysiological recordings were performed in slices derived from naïve WT littermates and the effects of amphetamine on striatopallidal IPSCs were assessed in control conditions or upon bath application of 10µM D2R antagonist sulpiride[80] (Tocris, UK, cat 0895). Paired-pulse ratio was calculated as previously described[80].

Quantifications and statistical analysis

All graphs and statistical analyses were performed using GraphPad software (version 8.0). Results were expressed as means of independent data points ± SEM. Student's t test and ANOVA (One-way or 2-way, where appropriate) analysis were performed and when interaction was significant Tukey's post hoc analysis was used. Post hoc significances were expressed as follow: * $p < 0.05$, ** $p < 0.01$, *** $p < 0.001$. Sample sizes, p values and statistical details can be found in **Table S1**.

REFERENCES LIST

1. Stewart, J., and Badiani, A. (1993). Tolerance and sensitization to the behavioral effects of drugs. Behavioural Pharmacology *4*, 289–312. 10.1097/00008877-199308000-00003.
2. Sequeira-Cordero, A., and Brenes, J.C. (2021). Time-dependent changes in striatal monoamine levels and gene expression following single and repeated amphetamine administration in rats. Eur J Pharmacol *904*. 10.1016/J.EJPHAR.2021.174148.
3. Thiemann, G., van der Stelt, M., Petrosino, S., Molleman, A., Di Marzo, V., and Hasenöhrl, R.U. (2008). The role of the CB1 cannabinoid receptor and its endogenous ligands, anandamide and 2-arachidonoylglycerol, in amphetamine-induced behavioural sensitization. Behavioural brain research *187*, 289–296. 10.1016/J.BBR.2007.09.022.
4. Davis, M.I., Crittenden, J.R., Feng, A.Y., Kupferschmidt, D.A., Naydenov, A., Stella, N., Graybiel, A.M., and Lovinger, D.M. (2018). The cannabinoid-1 receptor is abundantly expressed in striatal striosomes and striosome-dendron bouquets of the substantia nigra. PLoS One *13*. 10.1371/JOURNAL.PONE.0191436.
5. Wood, S., Sage, J.R., Shuman, T., and Anagnostaras, S.G. (2014). Psychostimulants and Cognition: A Continuum of Behavioral and Cognitive Activation. Pharmacol Rev *66*, 193–221. 10.1124/pr.112.007054.
6. Minassian, A., Young, J.W., Cope, Z.A., Henry, B.L., Geyer, M.A., and Perry, W. (2016). Amphetamine increases activity but not exploration in humans and mice. Psychopharmacology (Berl) *233*, 225–233. 10.1007/s00213-015-4098-4.
7. Faraone, S. V. (2018). The pharmacology of amphetamine and methylphenidate: Relevance to the neurobiology of attention-deficit/hyperactivity disorder and other psychiatric comorbidities. Neurosci Biobehav Rev *87*, 255–270. 10.1016/j.neubiorev.2018.02.001.
8. Badiani, A., Belin, D., Epstein, D., Calu, D., and Shaham, Y. (2011). Opiate versus psychostimulant addiction: the differences do matter. Nat Rev Neurosci *12*, 685–700. 10.1038/nrn3104.
9. Sax, K.W., and Strakowski, S.M. (2001). Behavioral Sensitization in Humans. J Addict Dis *20*, 55–65. 10.1300/J069v20n03_06.
10. Robinson, T.E., and Berridge, K.C. (2001). Incentive-sensitization and addiction. Addiction *96*, 103–114. 10.1046/j.1360-0443.2001.9611038.x.

11. Robinson, T.E., and Badiani, A. (1997). Drug-Induced Adaptations in Catecholamine Systems: On the Inevitability of Sensitization. In, pp. 987–990. 10.1016/S1054-3589(08)60912-6.
12. Pantoni, M.M., Kim, J.L., Van Alstyne, K.R., and Anagnostaras, S.G. (2022). MDMA and memory, addiction, and depression: dose-effect analysis. Psychopharmacology (Berl) *239*, 935–949. 10.1007/s00213-022-06086-9.
13. Deroche, V., Le Moal, M., and Piazza, P.V. (1999). Cocaine self-administration increases the incentive motivational properties of the drug in rats. European Journal of Neuroscience *11*, 2731–2736. 10.1046/j.1460-9568.1999.00696.x.
14. London, E.D. (2016). Impulsivity, Stimulant Abuse, and Dopamine Receptor Signaling. In, pp. 67–84. 10.1016/bs.apha.2016.01.002.
15. Fleckenstein, A.E., Volz, T.J., Riddle, E.L., Gibb, J.W., and Hanson, G.R. (2007). New Insights into the Mechanism of Action of Amphetamines. Annu Rev Pharmacol Toxicol *47*, 681–698. 10.1146/annurev.pharmtox.47.120505.105140.
16. Paulson, P.E., and Robinson, T.E. (1995). Amphetamine-Induced time-dependent sensitization of dopamine neurotransmission in the dorsal and ventral striatum: A microdialysis study in behaving rats. Synapse *19*, 56–65. 10.1002/syn.890190108.
17. Vanderschuren, L.J.M.J., Schoffelmeer, A.N.M., Van Leeuwen, S.D.C., Hof, L., Jonker, A.J., and Voorn, P. (2002). Compartment-specific changes in striatal neuronal activity during expression of amphetamine sensitization are the result of drug hypersensitivity. European Journal of Neuroscience *16*, 2462–2468. 10.1046/j.1460-9568.2002.02308.x.
18. Surmeier, D.J., Ding, J., Day, M., Wang, Z., and Shen, W. (2007). D1 and D2 dopamine-receptor modulation of striatal glutamatergic signaling in striatal medium spiny neurons. Trends Neurosci *30*, 228–235. 10.1016/j.tins.2007.03.008.
19. Bateup, H.S., Santini, E., Shen, W., Birnbaum, S., Valjent, E., Surmeier, D.J., Fisone, G., Nestler, E.J., and Greengard, P. (2010). Distinct subclasses of medium spiny neurons differentially regulate striatal motor behaviors. Proceedings of the National Academy of Sciences *107*, 14845–14850. 10.1073/pnas.1009874107.
20. Klaus, A., Alves da Silva, J., and Costa, R.M. (2019). What, If, and When to Move: Basal Ganglia Circuits and Self-Paced Action Initiation. Annu Rev Neurosci *42*, 459–483. 10.1146/annurev-neuro-072116-031033.
21. Cui, G., Jun, S.B., Jin, X., Pham, M.D., Vogel, S.S., Lovinger, D.M., and Costa, R.M. (2013). Concurrent activation of striatal direct and indirect pathways during action initiation. Nature *494*, 238–242. 10.1038/nature11846.

22. Calabresi, P., Picconi, B., Tozzi, A., Ghiglieri, V., and Di Filippo, M. (2014). Direct and indirect pathways of basal ganglia: a critical reappraisal. Nat Neurosci *17*, 1022–1030. 10.1038/nn.3743.
23. Prager, E.M., and Plotkin, J.L. (2019). Compartmental function and modulation of the striatum. J Neurosci Res, jnr.24522. 10.1002/jnr.24522.
24. Allichon, M.-C., Ortiz, V., Pousinha, P., Andrianarivelo, A., Petitbon, A., Heck, N., Trifilieff, P., Barik, J., and Vanhoutte, P. (2021). Cell-Type-Specific Adaptions in Striatal Medium-Sized Spiny Neurons and Their Roles in Behavioral Responses to Drugs of Abuse. Front Synaptic Neurosci *13*. 10.3389/fnsyn.2021.799274.
25. Ferguson, S.M., Eskenazi, D., Ishikawa, M., Wanat, M.J., Phillips, P.E.M., Dong, Y., Roth, B.L., and Neumaier, J.F. (2011). Transient neuronal inhibition reveals opposing roles of indirect and direct pathways in sensitization. Nat Neurosci *14*, 22–24. 10.1038/nn.2703.
26. Bonm, A. V., Elezgarai, I., Gremel, C.M., Viray, K., Bamford, N.S., Palmiter, R.D., Grandes, P., Lovinger, D.M., and Stella, N. (2021). Control of exploration, motor coordination and amphetamine sensitization by cannabinoid CB 1 receptors expressed in medium spiny neurons. European Journal of Neuroscience *54*, 4934–4952. 10.1111/ejn.15381.
27. Corbille, A.-G., Valjent, E., Marsicano, G., Ledent, C., Lutz, B., Herve, D., and Girault, J.-A. (2007). Role of Cannabinoid Type 1 Receptors in Locomotor Activity and Striatal Signaling in Response to Psychostimulants. Journal of Neuroscience *27*, 6937–6947. 10.1523/JNEUROSCI.3936-06.2007.
28. Deng, L., Viray, K., Singh, S., Cravatt, B., and Stella, N. (2022). ABHD6 Controls Amphetamine-Stimulated Hyperlocomotion: Involvement of CB 1 Receptors. Cannabis Cannabinoid Res *7*, 188–198. 10.1089/can.2021.0066.
29. Julian, M.D., Martin, A.B., Cuellar, B., Rodriguez De Fonseca, F., Navarro, M., Moratalla, R., and Garcia-Segura, L.M. (2003). Neuroanatomical relationship between type 1 cannabinoid receptors and dopaminergic systems in the rat basal ganglia. Neuroscience *119*, 309–318. 10.1016/S0306-4522(03)00070-8.
30. Marsicano, G., Goodenough, S., Monory, K., Hermann, H., Eder, M., Cannich, A., Azad, S.C., Cascio, M.G., Gutiérrez, S.O., van der Stelt, M., et al. (2003). CB1 Cannabinoid Receptors and On-Demand Defense Against Excitotoxicity. Science (1979) *302*, 84–88. 10.1126/science.1088208.
31. Gong, S., Doughty, M., Harbaugh, C.R., Cummins, A., Hatten, M.E., Heintz, N., and Gerfen, C.R. (2007). Targeting Cre Recombinase to Specific Neuron Populations with Bacterial Artificial Chromosome Constructs. Journal of Neuroscience *27*, 9817–9823. 10.1523/JNEUROSCI.2707-07.2007.

32. Gerfen, C.R., Paletzki, R., and Heintz, N. (2013). GENSAT BAC Cre-Recombinase Driver Lines to Study the Functional Organization of Cerebral Cortical and Basal Ganglia Circuits. Neuron *80*, 1368–1383. 10.1016/j.neuron.2013.10.016.
33. Ruud, J., Alber, J., Tokarska, A., Engström Ruud, L., Nolte, H., Biglari, N., Lippert, R., Lautenschlager, Ä., Cieślak, P.E., Szumiec, Ł., et al. (2019). The Fat Mass and Obesity-Associated Protein (FTO) Regulates Locomotor Responses to Novelty via D2R Medium Spiny Neurons. Cell Rep *27*, 3182-3198.e9. 10.1016/j.celrep.2019.05.037.
34. Wang, Q., and Zhou, F.M. (2019). cAMP-producing chemogenetic and adenosine A2a receptor activation inhibits the inwardly rectifying potassium current in striatal projection neurons. Neuropharmacology *148*, 229–243. 10.1016/j.neuropharm.2019.01.014.
35. Crittenden, J.R., Yoshida, T., Venu, S., Mahar, A., and Graybiel, A.M. (2022). Cannabinoid Receptor 1 Is Required for Neurodevelopment of Striosome-Dendron Bouquets. eNeuro *9*. 10.1523/ENEURO.0318-21.2022.
36. Gerfen, C.R., Baimbridget, K.G., and Millert, J.J. (1985). The neostriatal mosaic: Compartmental distribution of calcium-binding protein and parvalbumin in the basal ganglia of the rat and monkey (striatal compartments/substantla nigra/dopamine). Neurobiology *82*, 8780–8784.
37. Lafenêtre, P., Chaouloff, F., and Marsicano, G. (2007). The endocannabinoid system in the processing of anxiety and fear and how CB1 receptors may modulate fear extinction. Pharmacol Res *56*, 367–381. 10.1016/j.phrs.2007.09.006.
38. Busquets-Garcia, A., Desprez, T., Metna-Laurent, M., Bellocchio, L., Marsicano, G., and Soria-Gomez, E. (2015). Dissecting the cannabinergic control of behavior: The where matters. BioEssays *37*, 1215–1225. 10.1002/bies.201500046.
39. Ohno-Shosaku, T., Tanimura, A., Hashimotodani, Y., and Kano, M. (2012). Endocannabinoids and Retrograde Modulation of Synaptic Transmission. The Neuroscientist *18*, 119–132. 10.1177/1073858410397377.
40. Castillo, P.E., Younts, T.J., Chávez, A.E., and Hashimotodani, Y. (2012). Endocannabinoid Signaling and Synaptic Function. Neuron *76*, 70–81. 10.1016/j.neuron.2012.09.020.
41. Ruehle, S., Remmers, F., Romo-Parra, H., Massa, F., Wickert, M., Wortge, S., Haring, M., Kaiser, N., Marsicano, G., Pape, H.-C., et al. (2013). Cannabinoid CB1 Receptor in Dorsal Telencephalic Glutamatergic Neurons: Distinctive Sufficiency for Hippocampus-Dependent and Amygdala-Dependent Synaptic and Behavioral Functions. Journal of Neuroscience *33*, 10264–10277. 10.1523/JNEUROSCI.4171-12.2013.

42. Soria-Gómez, E., Bellocchio, L., Reguero, L., Lepousez, G., Martin, C., Bendahmane, M., Ruehle, S., Remmers, F., Desprez, T., Matias, I., et al. (2014). The endocannabinoid system controls food intake via olfactory processes. Nat Neurosci *17*, 407–415. 10.1038/nn.3647.
43. Soria-Gomez, E., Pagano Zottola, A.C., Mariani, Y., Desprez, T., Barresi, M., Bonilla-del Río, I., Muguruza, C., Le Bon-Jego, M., Julio-Kalajzić, F., Flynn, R., et al. (2021). Subcellular specificity of cannabinoid effects in striatonigral circuits. Neuron *109*, 1513-1526.e11. 10.1016/j.neuron.2021.03.007.
44. Metna-Laurent, M., Mondésir, M., Grel, A., Vallée, M., and Piazza, P. (2017). Cannabinoid-Induced Tetrad in Mice. Curr Protoc Neurosci *80*. 10.1002/cpns.31.
45. Cole, R.L., Konradi, C., Douglass, J., and Hyman, S.E. (1995). Neuronal adaptation to amphetamine and dopamine: Molecular mechanisms of prodynorphin gene regulation in rat striatum. Neuron *14*, 813–823. 10.1016/0896-6273(95)90225-2.
46. DeLong, M.R., and Wichmann, T. (2007). Circuits and Circuit Disorders of the Basal Ganglia. Arch Neurol *64*, 20. 10.1001/archneur.64.1.20.
47. Vanderschuren, L.J.M.J., Schoffelmeer, A.N.M., Van Leeuwen, S.D.C., Hof, L., Jonker, A.J., and Voorn, P. (2002). Compartment-specific changes in striatal neuronal activity during expression of amphetamine sensitization are the result of drug hypersensitivity. European Journal of Neuroscience *16*, 2462–2468. 10.1046/J.1460-9568.2002.02308.X.
48. Jedynak, J.P., Cameron, C.M., and Robinson, T.E. (2012). Repeated Methamphetamine Administration Differentially Alters Fos Expression in Caudate-Putamen Patch and Matrix Compartments and Nucleus Accumbens. PLoS One *7*, e34227. 10.1371/JOURNAL.PONE.0034227.
49. de Lera Ruiz, M., Lim, Y.-H., and Zheng, J. (2014). Adenosine A 2A Receptor as a Drug Discovery Target. J Med Chem *57*, 3623–3650. 10.1021/jm4011669.
50. Borea, P.A., Gessi, S., Merighi, S., Vincenzi, F., and Varani, K. (2018). Pharmacology of Adenosine Receptors: The State of the Art. Physiol Rev *98*, 1591–1625. 10.1152/physrev.00049.2017.
51. Zhao, Z., Soria-Gómez, E., Varilh, M., Covelo, A., Julio-Kalajzić, F., Cannich, A., Castiglione, A., Vanhoutte, L., Duveau, A., Zizzari, P., et al. (2020). A Novel Cortical Mechanism for Top-Down Control of Water Intake. Current Biology *30*, 4789-4798.e4. 10.1016/j.cub.2020.09.011.
52. Bogacz, R., Martin Moraud, E., Abdi, A., Magill, P.J., and Baufreton, J. (2016). Properties of Neurons in External Globus Pallidus Can Support Optimal Action Selection. PLoS Comput Biol *12*, e1005004. 10.1371/journal.pcbi.1005004.

53. Rommelfanger, K.S., and Wichmann, T. (2010). Extrastriatal dopaminergic circuits of the basal ganglia. Front Neuroanat. 10.3389/fnana.2010.00139.
54. Albin, R.L., Young, A.B., and Penney, J.B. (1989). The functional anatomy of basal ganglia disorders. Trends Neurosci *12*, 366–375. 10.1016/0166-2236(89)90074-X.
55. Ciriachi, C., Svane-Petersen, D., and Rickhag, M. (2019). Genetic tools to study complexity of striatal function. J Neurosci Res *97*, 1181–1193. 10.1002/jnr.24479.
56. Tecuapetla, F., Matias, S., Dugue, G.P., Mainen, Z.F., and Costa, R.M. (2014). Balanced activity in basal ganglia projection pathways is critical for contraversive movements. Nat Commun *5*, 4315. 10.1038/ncomms5315.
57. Di Chiara, G., and Imperato, A. (1988). Drugs abused by humans preferentially increase synaptic dopamine concentrations in the mesolimbic system of freely moving rats. Proceedings of the National Academy of Sciences *85*, 5274–5278. 10.1073/pnas.85.14.5274.
58. ROBINSON, T., and BECKER, J. (1986). Enduring changes in brain and behavior produced by chronic amphetamine administration: A review and evaluation of animal models of amphetamine psychosis. Brain Res *396*, 157–198. 10.1016/S0006-8993(86)80193-7.
59. Valverde, O., and Rodríguez-Árias, M. (2013). Modulation of 3,4-Methylenedioxymethamphetamine Effects by Endocannabinoid System. Curr Pharm Des *19*, 7081–7091. 10.2174/13816128194013120914433l.
60. Su, H., and Zhao, M. (2017). Endocannabinoid mechanism in amphetamine-type stimulant use disorders: A short review. Journal of Clinical Neuroscience *46*, 9–12. 10.1016/j.jocn.2017.08.042.
61. Magendzo, K., and Bustos, G. (2003). Expression of amphetamine-induced behavioral sensitization after short- and long-term withdrawal periods: Participation of μ- and δ-opioid receptors. Neuropsychopharmacology *28*, 468–477. 10.1038/sj.npp.1300063.
62. Hikida, T., Kimura, K., Wada, N., Funabiki, K., and Nakanishi, S. (2010). Distinct Roles of Synaptic Transmission in Direct and Indirect Striatal Pathways to Reward and Aversive Behavior. Neuron *66*, 896–907. 10.1016/j.neuron.2010.05.011.
63. Ketzef, M., and Silberberg, G. (2021). Differential Synaptic Input to External Globus Pallidus Neuronal Subpopulations In Vivo. Neuron *109*, 516-529.e4. 10.1016/j.neuron.2020.11.006.
64. Calabresi, P., Picconi, B., Tozzi, A., Ghiglieri, V., and Di Filippo, M. (2014). Direct and indirect pathways of basal ganglia: a critical reappraisal. Nat Neurosci *17*, 1022–1030. 10.1038/nn.3743.

65. Piette, C., Cui, Y., Gervasi, N., and Venance, L. (2020). Lights on Endocannabinoid-Mediated Synaptic Potentiation. Front Mol Neurosci *13*. 10.3389/fnmol.2020.00132.
66. Huang, Y.-C., Wang, S.-J., Chiou, L.-C., and Gean, P.-W. (2003). Mediation of Amphetamine-Induced Long-Term Depression of Synaptic Transmission by CB 1 Cannabinoid Receptors in the Rat Amygdala. The Journal of Neuroscience *23*, 10311–10320. 10.1523/JNEUROSCI.23-32-10311.2003.
67. Centonze, D., Battista, N., Rossi, S., Mercuri, N.B., Finazzi-Agrò, A., Bernardi, G., Calabresi, P., and Maccarrone, M. (2004). A Critical Interaction between Dopamine D2 Receptors and Endocannabinoids Mediates the Effects of Cocaine on Striatal GABAergic Transmission. Neuropsychopharmacology *29*, 1488–1497. 10.1038/sj.npp.1300458.
68. Giuffrida, A., Parsons, L.H., Kerr, T.M., de Fonseca, F.R., Navarro, M., and Piomelli, D. (1999). Dopamine activation of endogenous cannabinoid signaling in dorsal striatum. Nat Neurosci *2*, 358–363. 10.1038/7268.
69. Marsicano, G., Wotjak, C.T., Azad, S.C., Bisogno, T., Rammes, G., Cascio, M.G., Hermann, H., Tang, J., Hofmann, C., Zieglgänsberger, W., et al. (2002). The endogenous cannabinoid system controls extinction of aversive memories. Nature *418*, 530–534. 10.1038/nature00839.
70. Bellocchio, L., Lafenêtre, P., Cannich, A., Cota, D., Puente, N., Grandes, P., Chaouloff, F., Piazza, P.V., and Marsicano, G. (2010). Bimodal control of stimulated food intake by the endocannabinoid system. Nat Neurosci *13*, 281–283. 10.1038/nn.2494.
71. Terral, G., Busquets-Garcia, A., Varilh, M., Achicallende, S., Cannich, A., Bellocchio, L., Bonilla-Del Río, I., Massa, F., Puente, N., Soria-Gomez, E., et al. (2019). CB1 Receptors in the Anterior Piriform Cortex Control Odor Preference Memory. Current Biology *29*, 2455-2464.e5. 10.1016/j.cub.2019.06.041.
72. Oliveira da Cruz, J.F., Busquets-Garcia, A., Zhao, Z., Varilh, M., Lavanco, G., Bellocchio, L., Robin, L., Cannich, A., Julio-Kalajzić, F., Lesté-Lasserre, T., et al. (2020). Specific Hippocampal Interneurons Shape Consolidation of Recognition Memory. Cell Rep *32*, 108046. 10.1016/j.celrep.2020.108046.
73. Marsicano, G., and Lutz, B. (1999). Expression of the cannabinoid receptor CB1 in distinct neuronal subpopulations in the adult mouse forebrain. European Journal of Neuroscience *11*, 4213–4225. 10.1046/j.1460-9568.1999.00847.x.
74. Monory, K., Blaudzun, H., Massa, F., Kaiser, N., Lemberger, T., Schütz, G., Wotjak, C.T., Lutz, B., and Marsicano, G. (2007). Genetic Dissection of Behavioural and

Autonomic Effects of Δ9-Tetrahydrocannabinol in Mice. PLoS Biol *5*, e269. 10.1371/journal.pbio.0050269.

75. Vallée, M., Vitiello, S., Bellocchio, L., Hebert-Chatelain, E., Monlezun, S., Martin-Garcia, E., Kasanetz, F., Baillie, G.L., Panin, F., Cathala, A., et al. (2014). Pregnenolone can protect the brain from cannabis intoxication. Science *343*, 94–98. 10.1126/SCIENCE.1243985.
76. Busquets-Garcia, A., Oliveira da Cruz, J.F., Terral, G., Zottola, A.C.P., Soria-Gómez, E., Contini, A., Martin, H., Redon, B., Varilh, M., Ioannidou, C., et al. (2018). Hippocampal CB1 Receptors Control Incidental Associations. Neuron *99*, 1247-1259.e7. 10.1016/j.neuron.2018.08.014.
77. Robin, L.M., Oliveira da Cruz, J.F., Langlais, V.C., Martin-Fernandez, M., Metna-Laurent, M., Busquets-Garcia, A., Bellocchio, L., Soria-Gomez, E., Papouin, T., Varilh, M., et al. (2018). Astroglial CB1 Receptors Determine Synaptic D-Serine Availability to Enable Recognition Memory. Neuron *98*, 935-944.e5. 10.1016/j.neuron.2018.04.034.
78. Jaber, M., Cador, M., Dumartin, B., Normand, E., Stinus, L., and Bloch, B. (1995). Acute and chronic amphetamine treatments differently regulate neuropeptide messenger RNA levels and Fos immunoreactivity in rat striatal neurons. Neuroscience *65*, 1041–1050. 10.1016/0306-4522(94)00537-F.
79. Aristieta, A., Barresi, M., Azizpour Lindi, S., Barrière, G., Courtand, G., de la Crompe, B., Guilhemsang, L., Gauthier, S., Fioramonti, S., Baufreton, J., et al. (2021). A Disynaptic Circuit in the Globus Pallidus Controls Locomotion Inhibition. Current Biology *31*, 707-721.e7. 10.1016/j.cub.2020.11.019.
80. Corkrum, M., Covelo, A., Lines, J., Bellocchio, L., Pisansky, M., Loke, K., Quintana, R., Rothwell, P.E., Lujan, R., Marsicano, G., et al. (2020). Dopamine-Evoked Synaptic Regulation in the Nucleus Accumbens Requires Astrocyte Activity. Neuron *105*, 1036-1047.e5. 10.1016/J.NEURON.2019.12.026.

KRT

REAGENT or RESOURCE	SOURCE	IDENTIFIER
Antibodies		
HRP linked antibodies: anti-rabbit anti-mouse	Cell Signaling Technology	#7074; AB_2099233
Tubulin	Santa Cruz Biotechnology	#sc-69969; AB_1118882
Cannabinoid receptor-1	Frontier Science Co. Ltd	#CB1-Go-Af450; AB_2571530
Calbindin	Sigma Aldrich	#C9848; AB_476894
c-Fos	Synaptic Systems	#226 005; AB_2800522
Cannabinoid receptor-1	Abcam	#ab23703 AB_447623
Tubulin	Santa Cruz Biotechnology	#sc-69969; AB_1118882
Mu Opioid Receptor (MOR)	Abcam	ab134054; AB_10638544
FOXP2	Abcam	#ab16046; AB_2107107
NeutrAvidin Protein, DyLight 633	Thermo Fisher Scientific	#22844
Sheep Anti-Fluorescein-POD	Roche	#11426346910; AB_840257
Sheep Anti-Digoxigenin-POD	Roche	#11207733910; AB_514500
Anti-mouse Alexa 488	Thermo Fisher Scientific	#A-21202; AB_141607
Anti-guinea pig Alexa 488	Thermo Fisher Scientific	#A-11073; AB_2534117
Anti-rabbit Alexa 488	Thermo Fisher Scientific	#A-21206; AB_2535792
Anti-rabbit Alexa 594	Thermo Fisher Scientific	# A11012; AB_2534079
Bacterial and virus strains		
AAV-retro-hSyn1-EBFP2-FLPo	VVF of ZNZ	v151-retro
AAV-retro-hSyn1-EBFP2	VVF of ZNZ	v140-retro
AAV-hEF1a-dFRT-iCre-EGFP	VVF of ZNZ	v245-1
Chemicals, peptides, and recombinant proteins		
Amphetamine sulphate	Tocris	2813
THC	Pharm GmbH	#1098E100/10
Buprecare	Axience	
Lidor	Axience	
Metacam	Boehringer Ingelheim	
Exagon	Richter pharma	
KCl	Sigma-Aldrich	P3911
NaCl	Sigma-Aldrich	S9888
NaH_2PO_4	Sigma-Aldrich	52074
$NaHCO_3$	Sigma-Aldrich	S6014
$CaCl_2$	Sigma-Aldrich	21049
$MgCl_2$	Sigma-Aldrich	M8266
Sucrose	Sigma-Aldrich	S0389
Glucose	Sigma-Aldrich	G5767
HEPES	Sigma-Aldrich	54457
EGTA	Sigma-Aldrich	E3889
ATP-na+	Sigma-Aldrich	A2383

GTP-Na+	Sigma-Aldrich	51120
Phosphocreatine	Sigma-Aldrich	P7936
Biocytin	Sigma-Aldrich	B4261
NBQX disodium salt	Abcam	ab120046
D-AP5	Abcam	ab120003
Sulpiride	Tocris	0895
Critical commercial assays		
Clarity Western ECL	Bio-Rad	#1705060
Super Signal West Femto Maximum Sensitivity Substrate	Thermo Fisher Scientific	#34094
TSA Plus Fluorescein System	Akoya biosciences	#NEL741001KT
TSA Plus Cyanine 3 System	Akoya biosciences	#NEL744001KT
Experimental models: Organisms/strains		
C57BL/6-N mice	Janvier (France)	N/A
CB1-KO mice Cnr1tm1.1Ltz, CB1null	Neurocentre Magendie (France)	MGI:2182924
CB1-flox mice Cnr1tm1.2Ltz	Neurocentre Magendie (France)	MGI:3045419
Drd1-Cre mice Tg(Drd1a-cre)EY217Gsat/Mmucd	Neurocentre Magendie (France)	MGI: 6121366
Adora2a-Cre mice Tg(Adora2a-cre)KG139Gsat/Mmucd	Neurocentre Magendie (France)	MGI: 4361654
S-CB1 mice (Stop-CB1) Cnr1tm2Ltz	Neurocentre Magendie (France)	MGI: 5523992
Software and algorithms		
GraphPad prism 6.0, 8.0, 10.0	GraphPad Software	N/A
ImageLab 5.2.1	Bio-Rad Laboratories	N/A
Adobe Illustrator 2023	Adobe Systems	N/A
ImageJ (version 1.36)	NIH	N/A
Clampfit, pClamp 10.7	Molecular Devices	N/A
Camplex 10.3	Molecular Devices	N/A

Figure 1

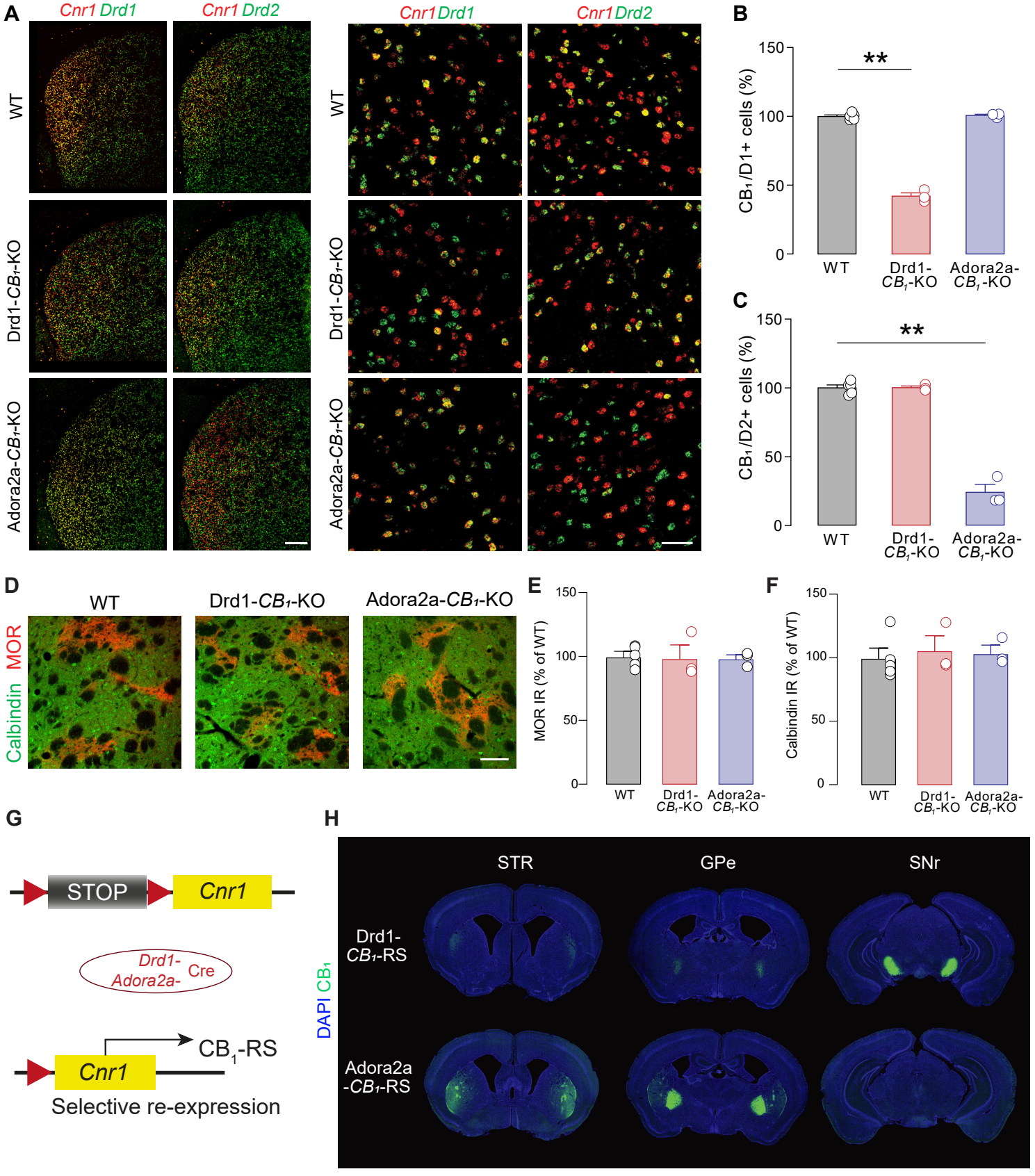
A
Cnr1 Drd1
Cnr1 Drd2
WT
Drd1-CB1-KO
Adora2a-CB1-KO
B
CB1/D1+ cells (%)
150
100
50
0
**
WT
Drd1-CB1-KO
Adora2a-CB1-KO
C
CB1/D2+ cells (%)
D
MOR
Calbindin
E
MOR IR (% of WT)
F
Calbindin IR (% of WT)
G
STOP
Cnr1
Drd1-
Adora2a-
Cre
CB1-RS
Selective re-expression
H
STR
GPe
SNr
DAPI CB1
Drd1-CB1-RS
Adora2a-CB1-RS

Figure 2

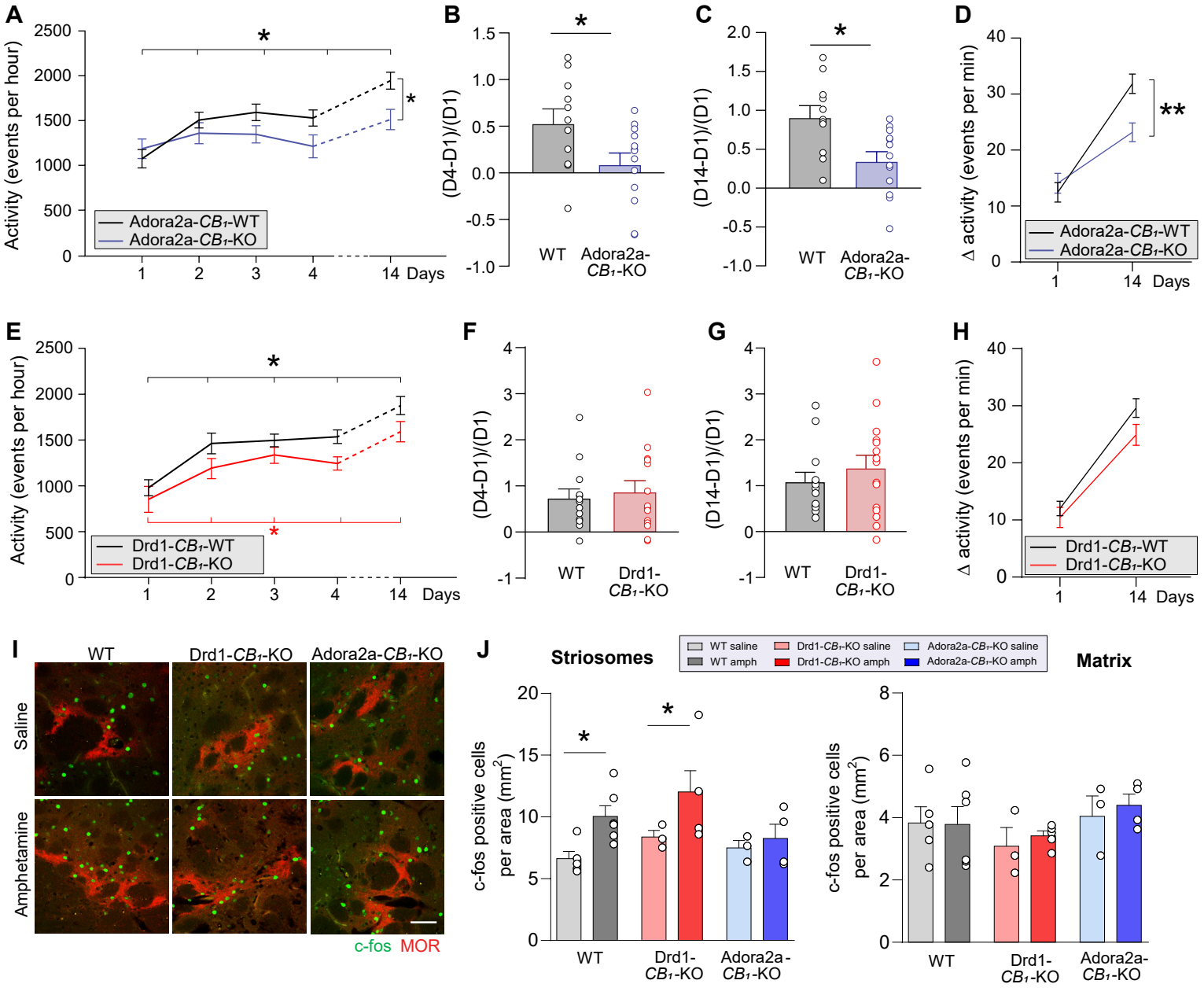
A
Activity (events per hour)
Adora2a-CB1-WT
Adora2a-CB1-KO
Days
B
(D4-D1)/(D1)
WT
Adora2a-CB1-KO
C
(D14-D1)/(D1)
D
Δ activity (events per min)
E
Drd1-CB1-WT
Drd1-CB1-KO
F
G
H
I
WT
Drd1-CB1-KO
Adora2a-CB1-KO
Saline
Amphetamine
c-fos MOR
J
Striosomes
Matrix
WT saline
WT amph
Drd1-CB1-KO saline
Drd1-CB1-KO amph
Adora2a-CB1-KO saline
Adora2a-CB1-KO amph
c-fos positive cells per area (mm2)

Figure 3

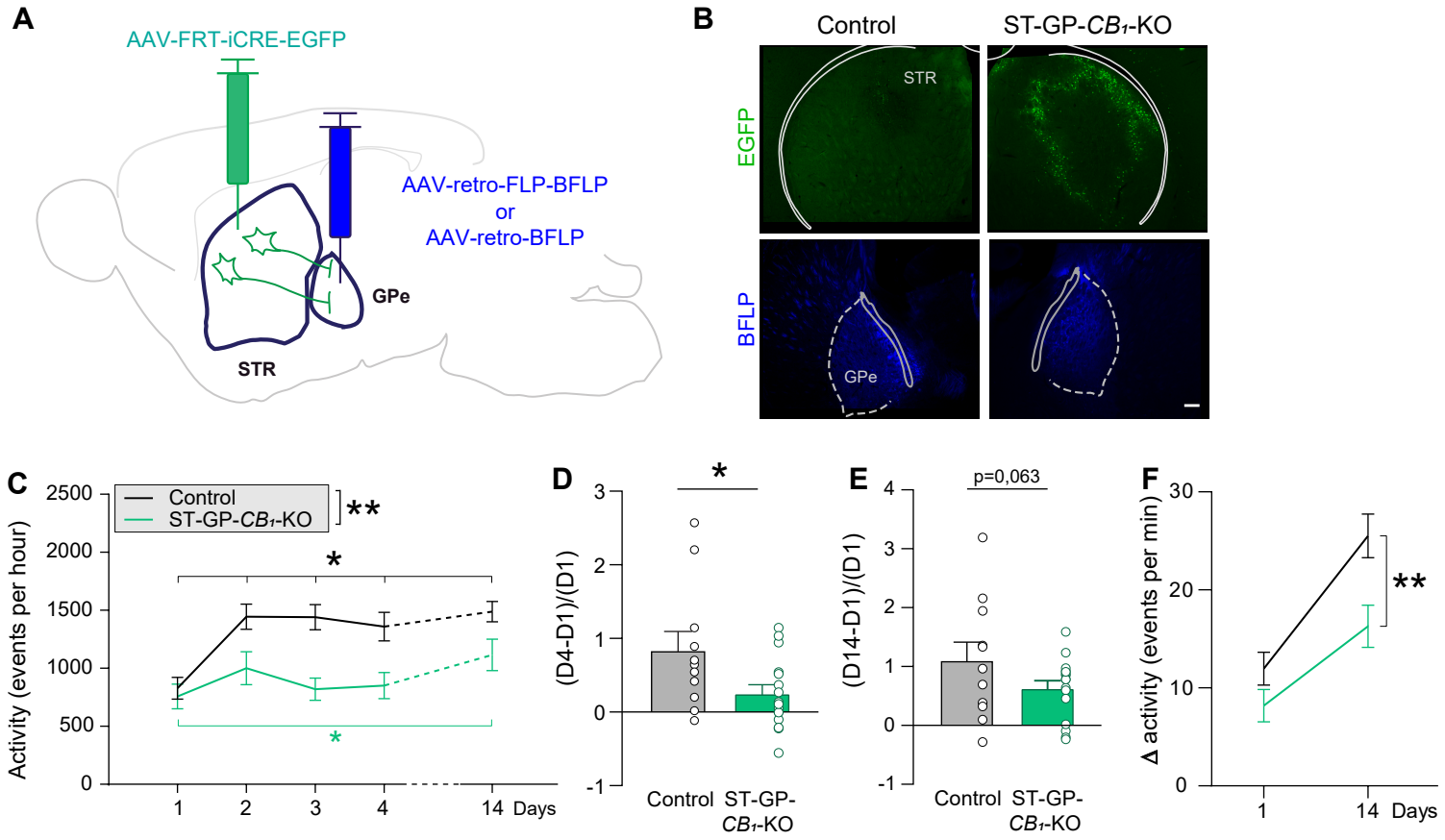
A
AAV-FRT-iCRE-EGFP
AAV-retro-FLP-BFLP
or
AAV-retro-BFLP
GPe
STR
B
Control
ST-GP-CB1-KO
STR
EGFP
BFLP
GPe
C
Control
ST-GP-CB1-KO
**
*
*
Activity (events per hour)
2500
2000
1500
1000
500
0
1
2
3
4
14 Days
D
*
(D4-D1)/(D1)
3
2
1
0
-1
Control
ST-GP-CB1-KO
E
p=0,063
(D14-D1)/(D1)
4
3
2
1
0
-1
Control
ST-GP-CB1-KO
F
Δ activity (events per min)
30
20
10
0
**
1
14 Days

Figure 4

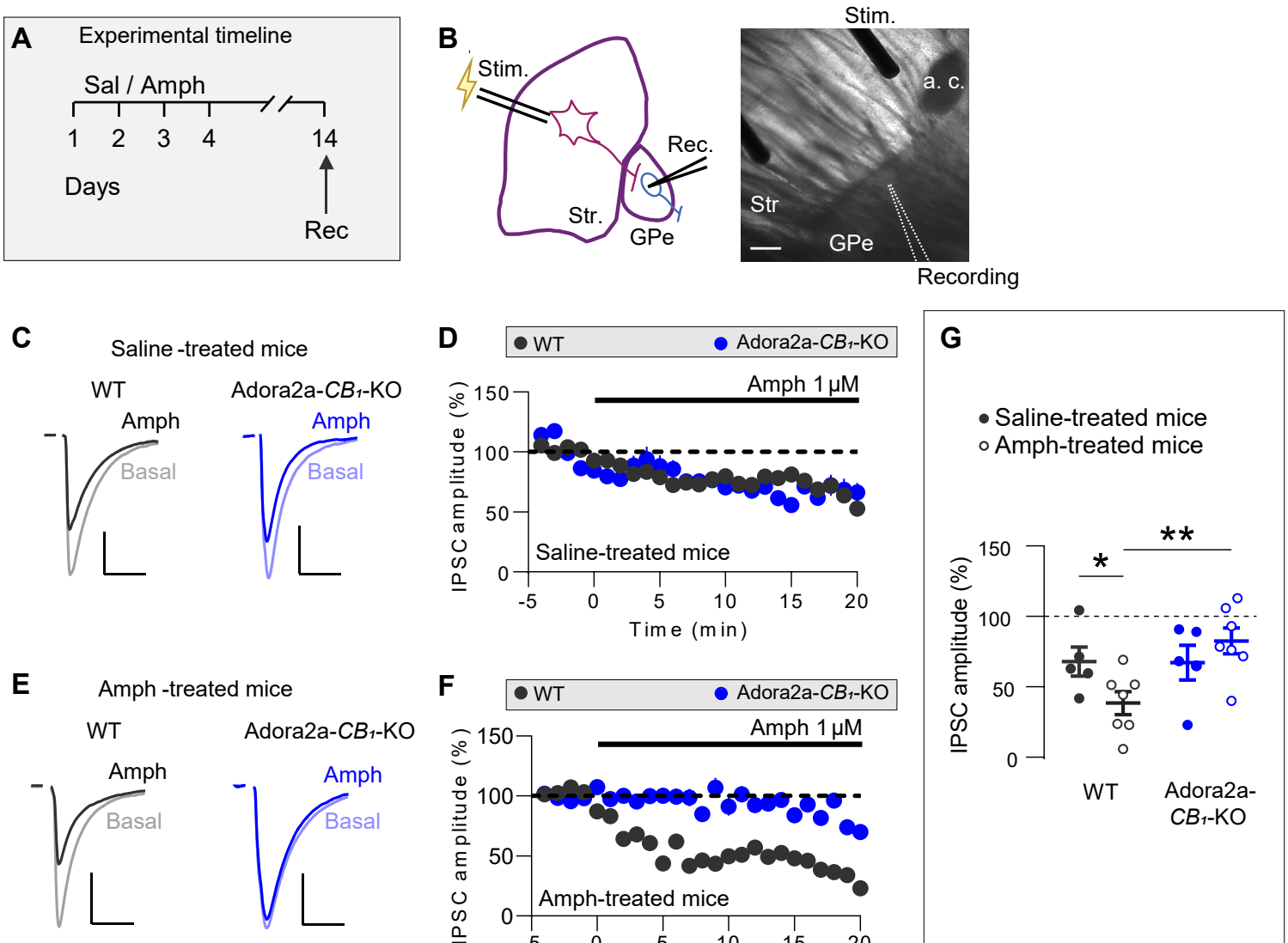
A
Experimental timeline
Sal / Amph
1 2 3 4 14
Days
Rec
B
Stim.
Rec.
Str.
GPe
Stim.
a. c.
Str
GPe
Recording
C
Saline -treated mice
WT
Adora2a-CB1-KO
Amph
Basal
Amph
Basal
D
WT
Adora2a-CB1-KO
Amph 1 μM
IPSC amplitude (%)
150
100
50
0
Saline-treated mice
-5 0 5 10 15 20
Time (min)
E
Amph -treated mice
WT
Adora2a-CB1-KO
Amph
Basal
Amph
Basal
F
WT
Adora2a-CB1-KO
Amph 1 μM
IPSC amplitude (%)
150
100
50
0
Amph-treated mice
-5 0 5 10 15 20
Time (min)
G
Saline-treated mice
Amph-treated mice
IPSC amplitude (%)
150
100
50
0
*
**
WT
Adora2a-CB1-KO

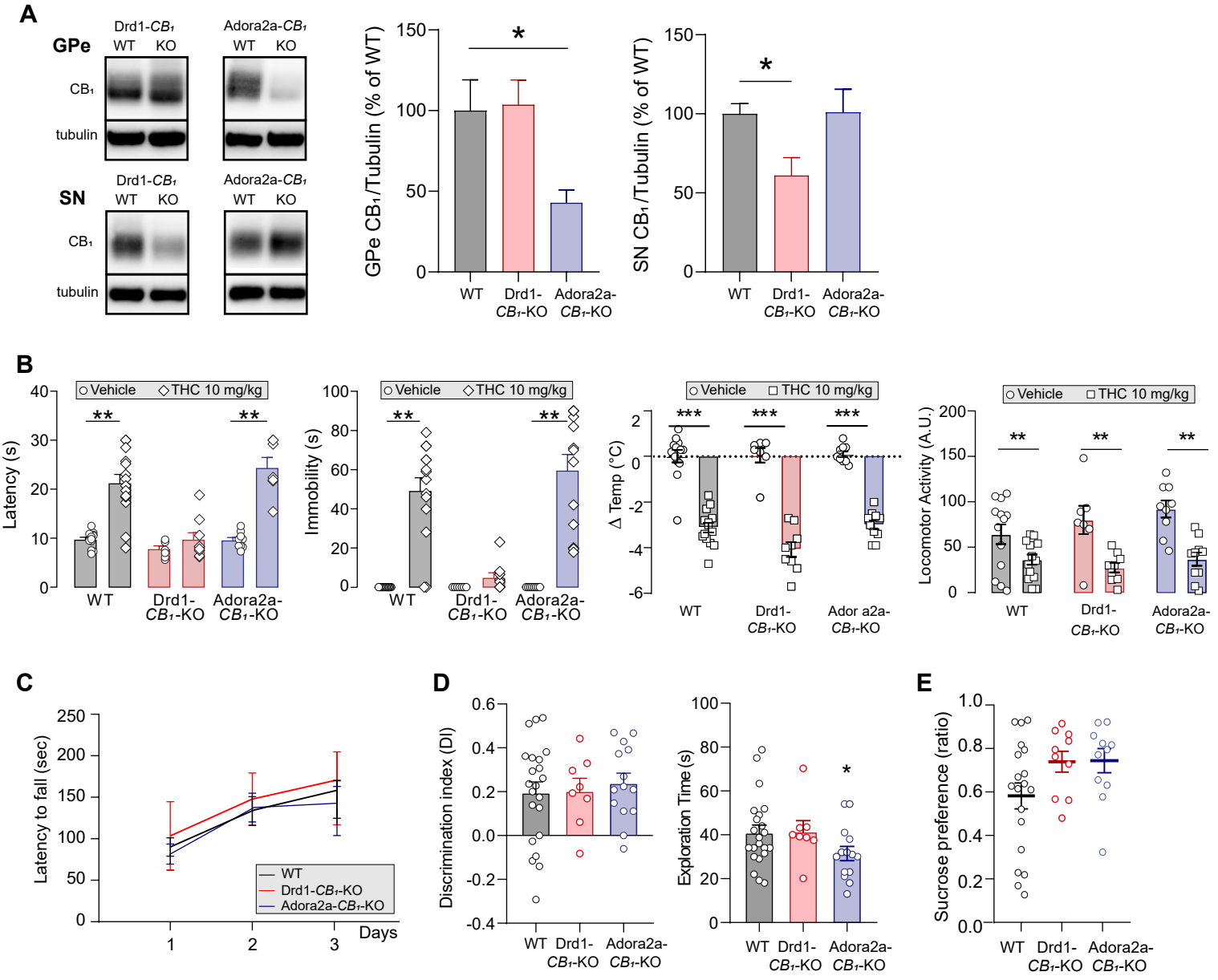

Figure S1. Conditional mutant mouse lines for studying striatal CB₁ receptors (related to Main Figure 1).

A) Representative immunoblot of CB₁ protein levels in the GPe and SN of Drd1-*CB₁*-KO and Adora2a-*CB₁*-KO mice; densitometric quantification of CB₁ levels in the GPe shows a significant reduction in Adora2a-CB₁-KO mice (left) and in the SN shows a significant reduction in Drd1-*CB₁*-KO mice (right). **B)** Tetrad behavior induced by THC (10 mg/kg i.p.); from the left: analgesia, catalepsy, hypotermia, and hypolocomotion in WT, Drd1-*CB₁*-KO, and Ado-ra2a-*CB₁*-KO mice. **C)** Rotarod test for eva-luating the motor coordation and motor skills learning. **D)** Memory performances tested by novel object recognition (NOR) test in mutant mice compare to WT littermates, discrimination index (left) and total exploration time (right). **E)** Sucrose preference calculated as the ration between sucrose consumption/total consumption over 1h of free-access to both drinking tubes. For statistics see **Table S1**.

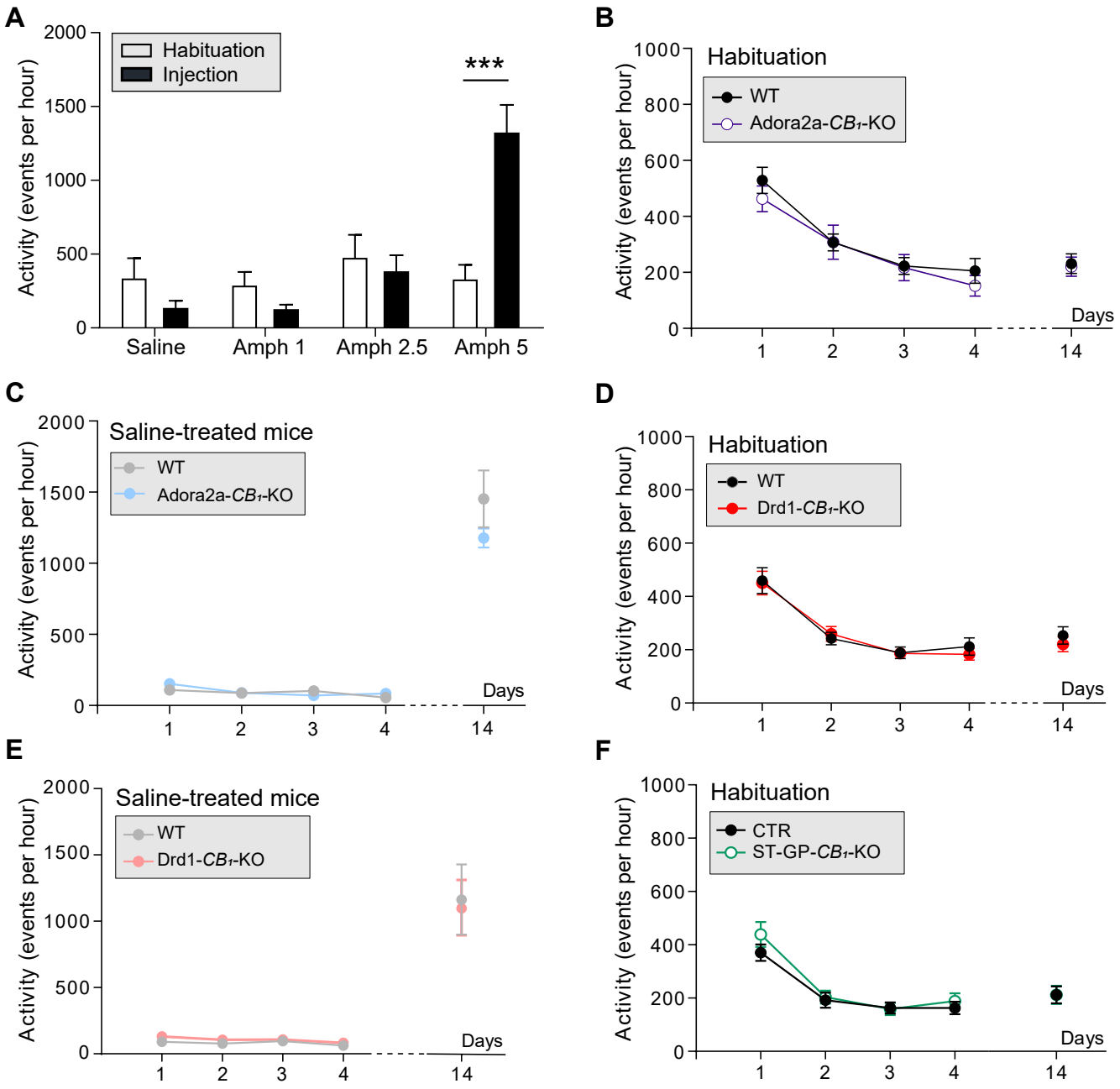

Figure S2. CB_1 receptors in striatopallidal neurons mediate amphetamine-induced sensitization (related to Main Figures 2-3).

A) Dose response of amphetamine injection on locomotory activity in WT naive mice. **B)** Basal locomotion of Adora2a-*CB₁*-KO mice and WT littermates; total activity recorded during the habituation phase (1h recording). **C)** Total activity of Adora2a-*CB₁*-KO and WT treated with saline during 4 days (Day 1 to day 4) and with amphetamine (5 mg/kg i.p.) at day 14. **D)** Basal locomotion of Drd1-*CB₁*-KO mice and WT littermates; total activity recorded during the habituation phase (1h recording). **E)** Total activity of Drd1-*CB₁*-KO and WT treated with saline during 4 days (Day 1 to day 4) and with amphetamine (5 mg/kg i.p.) at day 14. **F)** Basal locomotion of ST-GPe-*CB₁*-KO and control mice; total activity recorded during the habituation phase (1h recording). For statistics see **Table S1**.

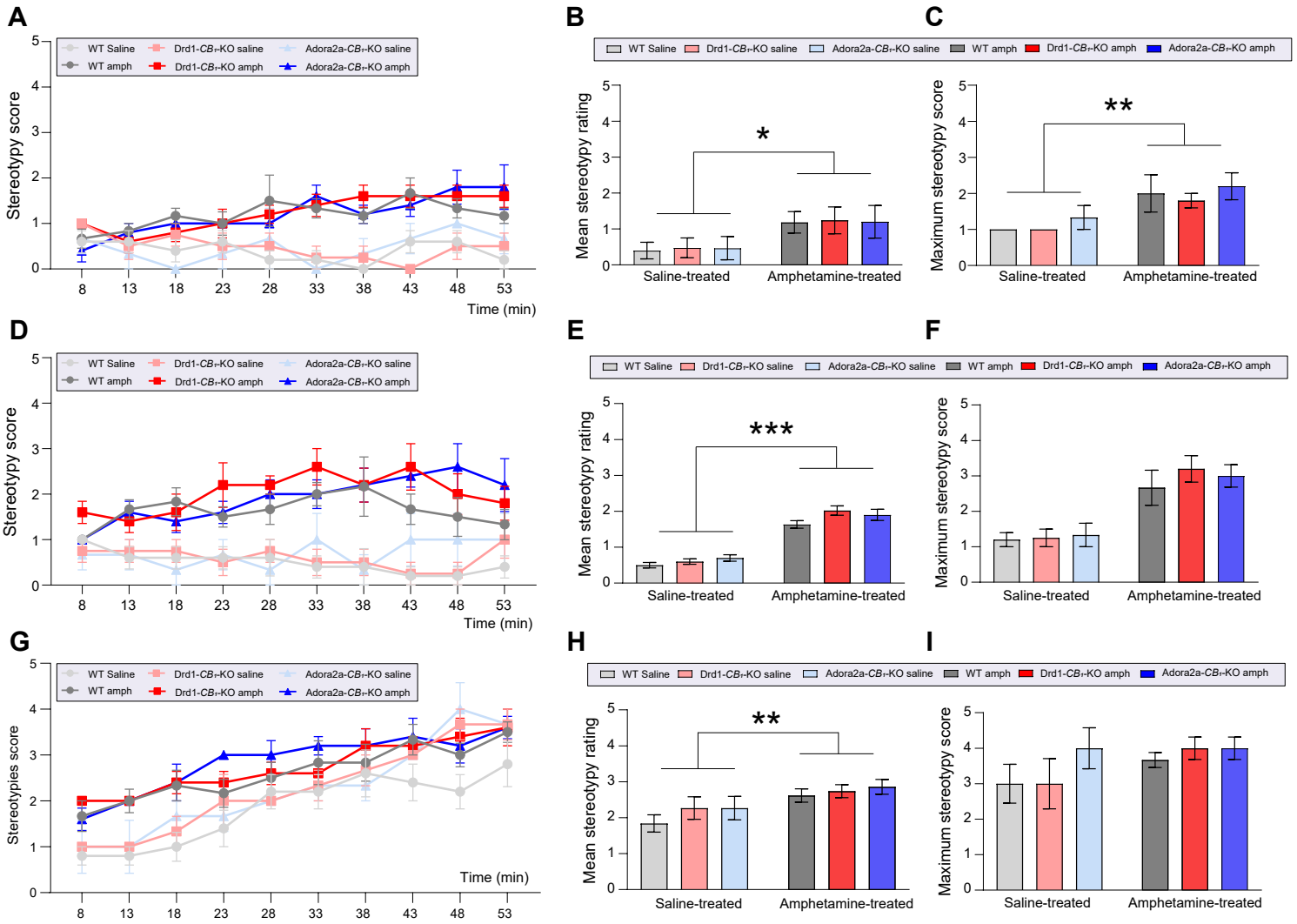

Figure S3. CB_1 receptor deletion in striatonigral and striatopallidal neurons does not influence amphetamine-induced stereotypies (related to Main Figure 2-3).

A) Timecourse after amphetamine treatment (5 mg/kg i.p.) at Day 1. **B)** Mean stereotypy rating and **C)** Maximum stereotypy score at Day 1 are significantly different in saline- and amphetamine-treated animals but show no differences between genotypes. **D)** Timecourse after amphetamine treatment (5 mg/kg i.p.) at Day 4. **E)** Mean stereotypy rating at Day 4 is significantly different in saline- and amphetamine-treated animals but show no differences between genotypes. **F)** Maximum stereotypy scores at Day 4 show no differences between treatment and genotypes. **G)** Timecourse after amphetamine treatment (5 mg/kg i.p.) at Day 14. **H)** Mean stereotypy rating at Day 14 is significantly different in saline- and amphetamine-treated animals but show no differen-ces between genotypes. **I)** Maximum stereotypy scores at Day 14 show no differences between treatment and genotypes. For statistics see **Table S1**.

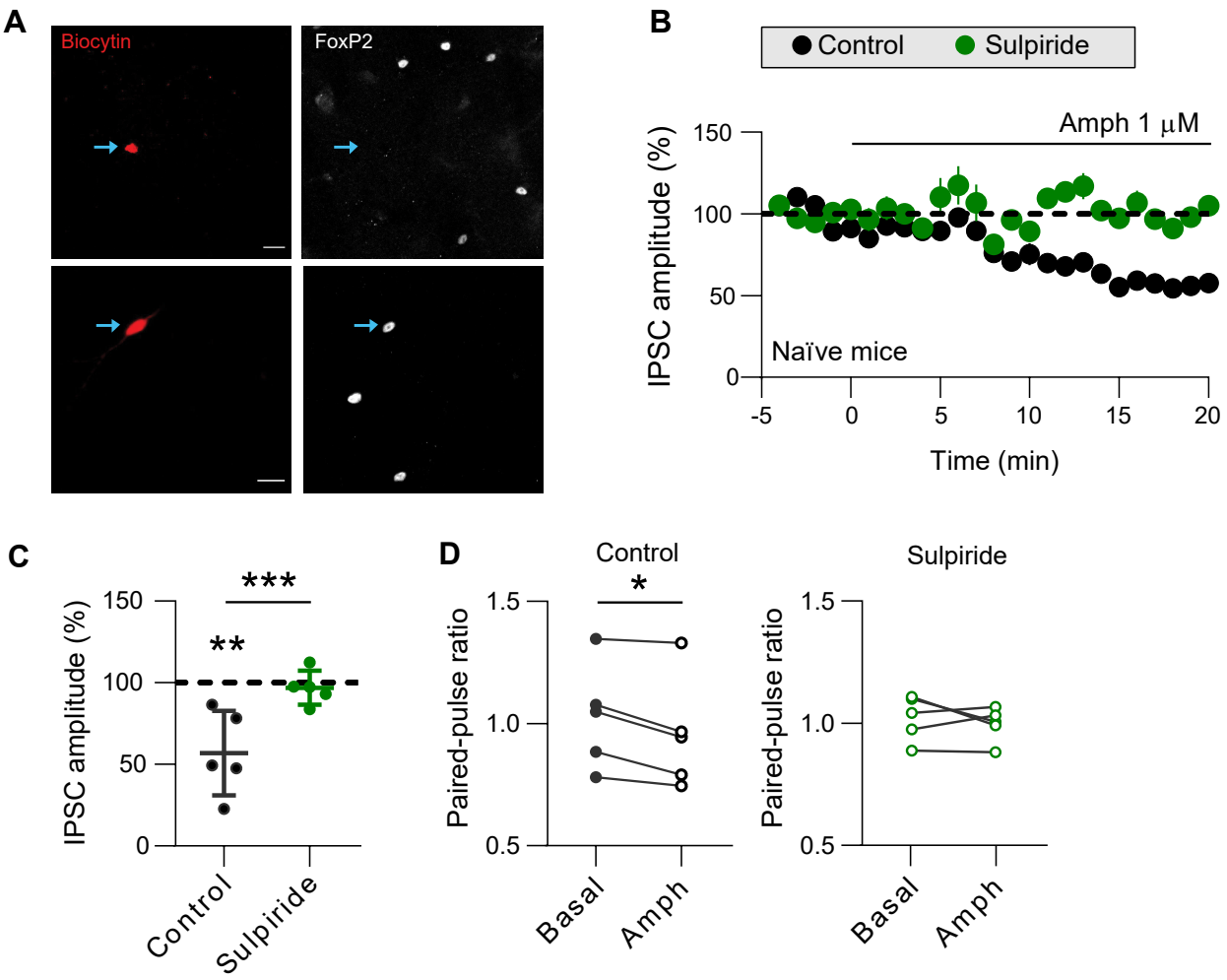

Figure S4. Repeated amphetamine exposure increases amphetamine-sensitivity of the striatopallidal pathway in a CB_1-dependent manner (related to main Figure 4). **A)** Immunofluorescence against FoxP2 (right) of biocytin filled neurons (left; arrow) after acute slice-recordings. Scale bar = 20 µm. **B)** Time course of bath-applied amphetamine on IPSC amplitude in naïve WT mice, in presence or not of D2 dopamine receptor antagonist sulpiride. **C)** Change in IPSC amplitude recorded 20 min after bath application of amphetamine. **D)** Change in paired-pulse ratio in CTR (left) and sulpiride (right) conditions recorded 20 min after bath application of amphetamine. For statistics see also **Table S1**.

	Conditions	"n" (x group)	Analysis (post-hoc reported in figure)	Factor analyzed	F Ratios	P value
1B	(WT vs Drd-*CB*$_1$-KO vs Adora2a-*CB*$_1$-KO) CB$_1$/D1+ cells	3-5	One way ANOVA (Kruskal-Wallis)		F (2, 8) = 483.9	P < 0.0001
1C	(WT vs Drd-*CB*$_1$-KO vs Adora2a-*CB*$_1$-KO) CB$_1$/D2+ cells	3-5	One way ANOVA (Kruskal-Wallis)		F (2, 8) = 173.7	P < 0.0001
1E	(WT vs Drd-*CB*$_1$-KO vs Adora2a-*CB*$_1$-KO) MOR	3-5	One way ANOVA (Kruskal-Wallis)		F (2, 8) = 0.01991	P = 0.9803
1F	(WT vs Drd-*CB*$_1$-KO vs Adora2a-*CB*$_1$-KO) Calbindin	3-5	One way ANOVA (Kruskal-Wallis)		F (2, 8) = 0.1303	P = 0.8797
2A	(WT vs Adora2a-*CB*$_1$-KO)	11-13	Two way ANOVA (Tukey)	GT x Time	Interaction F (4, 88) = 2.474 GT F (1, 88) = 9.148 Time F (4, 88) = 10.47	P = 0.0482 P = 0.0029 P < 0.0001
2B	(WT vs Adora2a-*CB*$_1$-KO) day4	11-13	t test			P =0.0288
2C	(WT vs Adora2a-*CB*$_1$-KO) day14	11-13	t test			P =0.0056
2D	(WT vs Adora2a-*CB*$_1$-KO)	11-13	Two way ANOVA (Tukey)	GT x Time	Interaction F (1, 44) = 6.378 GT F (1, 44) = 4.295 Time F (1, 44) = 59.95	P = 0.0151 P = 0.0498 P < 0.0001
2E	(WT vs Drd1-*CB*$_1$-KO)	13-15	Two way ANOVA (Tukey)	GT x Time	Interaction F (4, 100) = 0.6316 GT F (1, 25) = 4.210 Time F (4, 100) = 36.60	P = 0.6411 P = 0.0508 P < 0.0001
2F	(WT vs Drd1-*CB*$_1$-KO) day4	13-15	t test			P = 0.6807
2G	(WT vs Drd1-*CB*$_1$-KO) day14	13-15	t test			P = 0.3998
2H	(WT vs Drd1-*CB*$_1$-KO)	13-15	Two way ANOVA (Tukey)	GT x Time	Interaction F (1, 50) = 0.8810 GT F (1, 50) = 4.295 Time F (1, 50) = 92.42	P = 0.3524 P = 0.0656 P < 0.0001
2J	(WT vs Drd1-*CB*$_1$-KO vs Adora2A-*CB*$_1$-KO) Striosomes	3-6	Two way ANOVA (Tukey)	GT x Treatment	Interaction F (2, 20) = 0.8707 GT F (2, 20) = 2.108 Treatment F (1, 20) = 7.575	P = 0.4339 P = 0.1477 P = 0.0123
2J	(WT vs Drd1-*CB*$_1$-KO vs Adora2A-*CB*$_1$-KO) Matrix	3-6	Two way ANOVA (Tukey)	GT x Treatment	Interaction F (2, 20) = 0.8810 GT F (2, 20) = 1.560 Treatment F (1, 20) = 0.2488	P = 0.1052 P = 0.2347 P = 0.6233
3C	(Ctr vs ST-GPe-*CB*$_1$-KO)	11-16	Two way ANOVA (Tukey)	AAV x Time	Interaction F (4, 100) = 3.480 AAV F (1, 25) = 8.669 Time F (4, 100) = 12.24	P = 0.0105 P = 0.0069 P < 0.0001
3D	(Ctr vs ST-GPe-*CB*$_1$-KO) day4	11-16	t test			P =0.0311
3E	(Ctr vs ST-GPe-*CB*$_1$-KO) day14	11-16	t test			P =0.0629
3F	(Ctr vs ST-GP-CB1-KO)	11-16	Two way ANOVA (Tukey)	GT x Time	Interaction F (1, 25) = 2.850 GT F (1, 25) = 4.295 Time F (1, 25) = 92.42	P = 0.1038 P =0.0102 P < 0.0001
4G	Amphetamine effects (WT vs Adora2a-*CB*$_1$-KO)	6-7	Two way ANOVA (Tukey)	GT x Treatment	Interaction F (1, 21) = 6.328 GT F (1, 21) = 4.389 Treatment F (1, 21) = 0.8347	P = 0.0201 P = 0.0405 P = 0.3713
S1A	(WT vs Drd-*CB*$_1$-KO vs Adora2a-*CB*$_1$-KO) Gpe	4	One way ANOVA (Kruskal-Wallis)		F (2, 9) = 5.251	P = 0.0308
S1A	(WT vs Drd-*CB*$_1$-KO vs Adora2a-*CB*$_1$-KO) SN	8-14	One way ANOVA (Kruskal-Wallis)		F (2, 29) = 4.842	P = 0.0153
S1B	(WT vs Drd-*CB*$_1$-KO vs Adora2a-*CB*$_1$-KO) Antinociception	7-13	Two way ANOVA (Tukey)	GT x Treatment	Interaction F (2, 53) = 9.898 GT F (2, 53) = 17.24 Treatment F (1, 53) = 66.52	P = 0.0002 P < 0.0001 P < 0.0001
S1B	(WT vs Drd-*CB*$_1$-KO vs Adora2a-*CB*$_1$-KO) Catalepsy	10-13	Two way ANOVA (Tukey)	GT x Treatment	Interaction F (2, 59) = 11.68 GT F (2, 59) = 11.68 Treatment F (1, 59) = 68.87	P < 0.0001 P < 0.0001 P < 0.0001
S1B	(WT vs Drd-CB$_1$-KO vs Adora2a-*CB*$_1$-KO) Hypothermia	9-14	Two way ANOVA (Tukey)	GT x Treatment	Interaction F (2, 56) = 2.301 GT F (2, 56) = 2.380 Treatment F (1, 56) = 270.9	P = 0.1096 P = 0.1018 P < 0.0001
S1B	(WT vs Drd-CB$_1$-KO vs Adora2a-*CB*$_1$-KO) Hypolocomotion	9-14	Two way ANOVA (Tukey)	GT x Treatment	Interaction F (2, 56) = 1.536 GT F (2, 56) = 1.356 Treatment F (1, 56) = 35.37	P = 0.2241 P = 0.2634 P < 0.0001
S1C	(WT vs Drd-*CB*$_1$-KO vs Adora2a-*CB*$_1$-KO)	9-14	Two way ANOVA (Tukey)	GT x Time	Interaction F (4, 45) = 0.05116 GT F (2, 45) = 0.4382 Time F (2, 45) = 270.9	P = 0.9949 P = 0.6479 P = 0.0062
S1D	(WT vs Drd-*CB*$_1$-KO vs Adora2a-*CB*$_1$-KO) DI	8-22	One way ANOVA (Kruskal-Wallis)		F (2, 41) = 0.6792	P = 0.5126
S1D	(WT vs Drd-*CB*$_1$-KO vs Adora2a-*CB*$_1$-KO) Total Exploration	8-22	One way ANOVA (Kruskal-Wallis)		F (2, 41) = 3.777	P = 0.0312
S1E	(WT vs Drd-*CB*$_1$-KO vs Adora2a-*CB*$_1$-KO)	10-19	One way ANOVA (Kruskal-Wallis)		F (2, 37) = 2.554	P = 0.0914
S2A	(Habituation vs Amphetamine)	5	Two way ANOVA (Tukey)	Dose x Time	Interaction F (3, 16) = 15.33 Dose F (3.16) = 11.96 Time F (1, 16) = 3.325	P < 0.0001 P = 0.0002 P = 0.0870
S2B	(WT vs Adora2a-*CB*$_1$-KO)	11-13	Two way ANOVA (Tukey)	GT x Time	Interaction F (4, 88) = 0.8198 GT F (1, 22) = 0.2427 Time F (4, 88) = 51.29	P = 0.5159 P = 0.6271 P < 0.0001
S2C	(WT vs Adora2a-*CB*$_1$-KO)	6	Two way ANOVA (Tukey)	GT x Time	Interaction F (4, 40) = 2.046 GT F (1, 10) = 0.7986 Time F (4, 40) = 142.2	P = 0.1063 P = 0.3925 P < 0.0001
S2D	(WT vs Drd1-*CB*$_1$-KO)	13-15	Two way ANOVA (Tukey)	GT x Time	Interaction F (4, 100) = 0.3975 GT F (1, 25) = 0.6511 Time F (4, 100) = 39.77	P = 0.8100 P = 0.4273 P < 0.0001
S2E	(WT vs Drd1-*CB*$_1$-KO)	5-7	Two way ANOVA (Tukey)	GT x Time	Interaction F (4, 40) = 0.08666 GT F (1, 10) = 0.007996 Time F (4, 40) = 42.71	P = 0.9861 P = 0.9305 P < 0.0001
S2F	(Ctr vs ST-GPe-*CB*$_1$-KO)	11-16	Two way ANOVA (Tukey)	AAV x Time	Interaction F (4, 100) = 0.3325 AAV F (1, 25) = 0.2625 Time F (4, 100) = 46.09	P = 0.3326 P = 0.6129 P < 0.0001
S3B	(WT vs Drd-*CB*$_1$-KO vs Adora2a-*CB*$_1$-KO) day 1	9-14	Two way ANOVA (Tukey)	GT x Treatment	Interaction F (2, 21) = 0.002 GT F (2, 21) = 0.0184 Treatment F (1, 21) = 6.507	P = 0.9975 P = 0.9818 P = 0.0186
S3C	(WT vs Drd-*CB*$_1$-KO vs Adora2a-*CB*$_1$-KO) day 1	9-14	Two way ANOVA (Tukey)	GT x Treatment	Interaction F (2, 21) = 0.041 GT F (2, 21) = 0.4686 Treatment F (1, 21) = 8.495	P = 0.9598 P = 0.6323 P = 0.0083
S3E	(WT vs Drd-*CB*$_1$-KO vs Adora2a-*CB*$_1$-KO) day 4	9-14	Two way ANOVA (Tukey)	GT x Treatment	Interaction F (2, 21) = 0.7340 GT F (2, 21) = 2.7843 Treatment F (1, 21) = 152.1	P = 0.4919 P = 0.0847 P < 0.0001
S3F	(WT vs Drd-*CB*$_1$-KO vs Adora2a-*CB*$_1$-KO) day 4	9-14	Two way ANOVA (Tukey)	GT x Treatment	Interaction F (2, 21) = 0.1948 GT F (2, 21) = 0.3360 Treatment F (1, 21) =27.10	P = 0.8245 P = 0.7184 P < 0.0001
S3H	(WT vs Drd-*CB*$_1$-KO vs Adora2a-*CB*$_1$-KO) day 14	9-14	Two way ANOVA (Tukey)	GT x Treatment	Interaction F (2, 21) = 0.2291 GT F (2, 21) = 1.281 Treatment F (1, 21) = 10.10	P = 0.7992 P = 0.2986 P = 0.0045
S3I	(WT vs Drd-*CB*$_1$-KO vs Adora2a-*CB*$_1$-KO) day 14	9-14	Two way ANOVA (Tukey)	GT x Treatment	Interaction F (2, 21) = 0.6310 GT F (2, 21) = 1.307 Treatment F (1, 21) = 2.493	P = 0.5418 P = 0.2917 P = 0.1293
S4C	IPSCs Control vs Sulpiride	5	t test			P = 0.0123
S4D	Paired-Pulse ratio Control	5	Paired t test			P = 0.0205
S4D	Paired-Pulse ratio Sulpiride	5	Paired t test			P = 0.4814

Table S1- Statistical analysis related to Figures 1-4 and S1-S4